Remeis Sternwarte Bamberg

Diplomarbeit

Radiative transport in strongly magnetized accretion columns

Author:
Maximilian Kriebel

Supervisor:
Prof. Dr. Jörn Wilms

15.10.12

FRIEDRICH-ALEXANDER
UNIVERSITÄT
ERLANGEN-NÜRNBERG

ERLANGEN CENTRE
FOR ASTROPARTICLE
PHYSICS

Contents

Figure 1: A terrestrial aurora from space. Polar lights can be observed with naked eyes when charged particles illuminate the atmosphere in the polar region. The particles originate from Solar wind or coronal mass ejections.(courtesy NASA)

1 Introduction

What has an aurora to do with the content of this work? In strong magnetic fields, the movement of charged particles is dominated by the Lorentz force (e.g Landau & Lifschitz, a).

$$m\frac{d\vec{v}}{dt} = \frac{e}{c}\vec{v} \times \vec{B} \tag{1}$$

The Lorentz force accelerates particles perpendicular to the magnetic field and perpendicular to their velocity. This forces them to move in circles. Parallel to the field the particles can move free, so they spiral along the magnetic field lines to the poles of the Earth, another planet or a moon.
This thesis is about the accretion of ionized matter to the poles of a neutron star or more precisely, about the interaction of radiation with the accreted matter. Also in strong magnetic fields, the quantum nature of particles get apparent in resonant interaction effects.

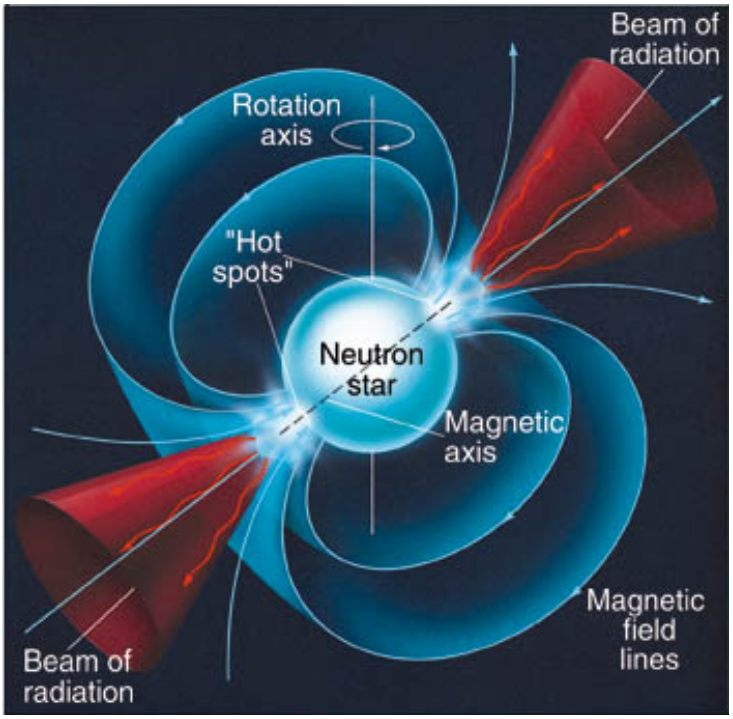

Figure 2: Magnetic field structure of an isolated neutron star(Chaisson, 2005, Fig. 22.3).

1.1 Neutron Stars

A star exists in permanent equilibrium of gravitational pressure pulling inwards and radiative pressure pushing outwards. The radiative pressure is generated by photons propagating in the star. The energy for these photons is provided by nuclear fusion in the core of the star. It depends on the mass of a star which elements it can merge to heavier elements. When the pressure in a star is not high enough to merge atoms available, no radiative pressure is provided anymore and only the degeneracy pressure of electrons withstands gravity(Meszaros, 1992). The carcass of our sun will be this stadium, a white dwarf.

If the progenitor mass of the star and therefore its gravitational pressure is high enough to dominate the degeneracy pressure electrons get pressed into the protons of their atoms and the core collapses. This process of electron proton neutralisation is called inverse β-decay and produces a neutron and an electron neutrino (Stöcker). The collapse of the core therefore emits a large amount of neutrinos. The hull falls towards the core which raises its density and temperature. These neutrinos together with a shock-wave, generated by a yet uncertain core back-bounce, then push the hull away (Meszaros, 1992). This death of a star is called type II supernova nova and forms a neutron star directly. another scenario is when a white dwarf accretes matter till it reaches the critical mass and collapses. These events are called type I supernovae (Meszaros, 1992, Chap. 11).

Neutron stars were first theoretically predicted in 1930 (Chandrasekhar, 1931) and observed in 1968 as periodically pulsating radio source (Hewish et al., 1968). An approximate lower boundary for the mass of neutron stars gives us the Chandrasekhar mass $M_{Ch} \approx 1.45 M_\odot$ (Meszaros, 1992, 1.2.6). Not exactly known is the upper border $3M_\odot \lesssim M_{\max} \lesssim 5M_\odot$ (Meszaros, 1992, 1.2.7), which is derived by the same princi-

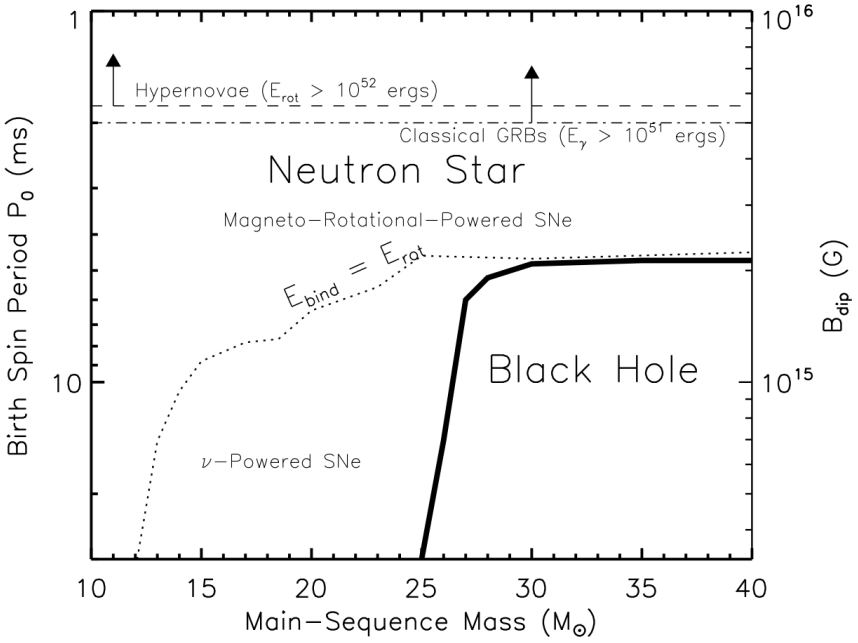

Figure 3: The picture is taken from (Metzger et al., 2011) and shows the expected fate of a star dependent of the mass and circular momentum. The created compact object can also be black hole depending on its progenitor mass and birth spin period.

ple comparing gravitational pressure with degeneracy pressure (Oppenheimer & Volkoff, 1939). The degenerated electron gas opposes gravity in a white dwarf. The degenerate neutron gas does the job in an neutron star. The radius of a neutron star of $M = 1.45 M_\odot$ can be approximated with (Meszaros, 1992, 1.2.11):

$$R \approx 4.5 \hbar^2 G^{-1} m_{\mathrm{p}}^{-\frac{8}{3}} M^{-\frac{1}{3}} \approx 1.2 \cdot 10^4 m \tag{2}$$

The assumed magnetic field strength at the surface of a neutron star is $\sim 10^{12}G$-$10^{13}G$ (Meszaros, 1992, Sect. 1.2.15). It can be explained with the conservation of magnetic field energy. The conservation of angular momentum while the collapse of the core can lead to very low spin periods of milliseconds.

The radiative output of an accreting neutron star or accretion powered source is powered by potential energy, which is provided when material falls towards the neutron star. Due to the high magnetic field of neutron stars, ionized material is being channeled in a very compact accretion column to the surface. The acellerated charges permanent emit Bremsstrahlung while falling towards the neutron star and then create luminous "hot spots" at the poles (Fig. 2). Again, because the magnetic axis and the rotation axis are not parallel, the luminous surface area an observer can see varies periodically over time which results in pulsations. The matter originates from different sources. It can be donated for example by the wind of luminous companion or if the hull of the companion overflows its Roche lobe, which is the point of gravitational equilibrium between the stars. If the radiative output of a neutron star is powered by its changing magnetic momentum its called rotation powered neutron star. Charges, currents, or magnetic moments are the sources of electromagnetic fields. If charges get acellerated or magnetic momenta change, test particles cannot feel the new field instantaneously, it needs the time $t = \frac{distance}{c}$.

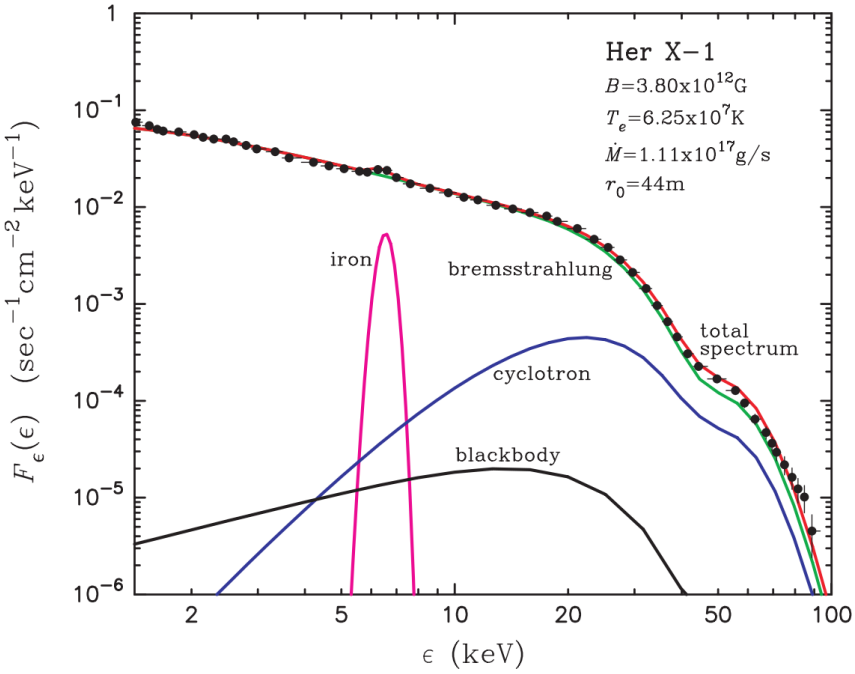

Figure 4: The picture is taken from (Becker & Wolff, 2007). The spectral emission of neutron stars can be modeled with iron fluorescence and a blackbody spectrum which is modified by resonant cyclotron scattering and emission. The spectrum in general is dominated by Bremsstrahlung, which originates from accelerated charged particles.

A way to construct electromagnetic waves out of a time dependent charge or current distribution are delayed potentials (Landau & Lifschitz, a). This change of field spreads with light-speed, carries energy away and therefore is called Bremsstrahlung.

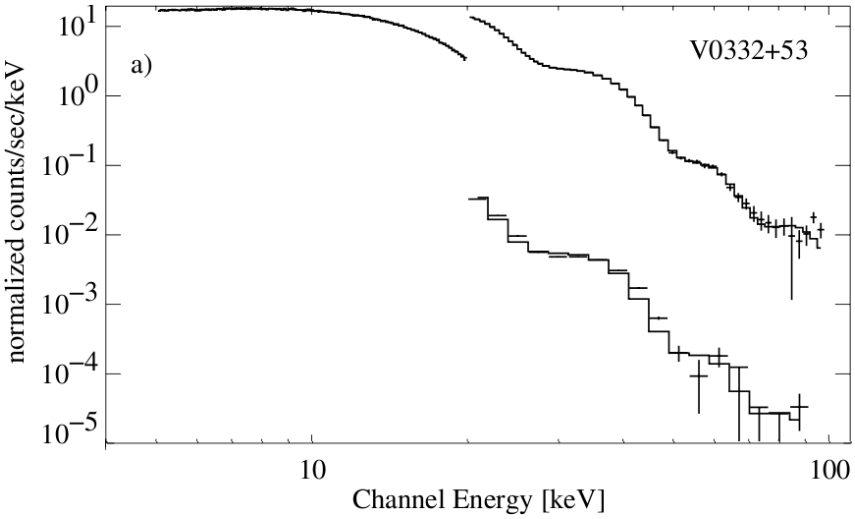

Figure 5: The plot is taken from (Kreykenbohm et al., 2005). It shows raw data of an outburst of V0332+53 and is obtained with all instruments on board the INTEGRAL satellite. In the raw data, three absorption features at 24.9keV, 50.5keV and 71.7keV are nearly visible.

1.2 Cyclotron lines

If the classical idea of continuously emitted Bremsstrahlung would be true, the electrons in atoms, which are accelerated permanently, would loose their energy to fast (Landau & Lifschitz, b). In fact, they emit energy packets in $\frac{eB}{mc}\hbar$. An electron can therefore reach a state where it does not have enough energy to emit, the ground state. As in atoms, electrons in strong magnetic fields also can only occupy discrete amounts of energy. These quantized electron states are called Landau levels. A Landau electron can absorb, or emit only photons near the electron cyclotron energy, which is:

$$\hbar\omega_{\mathrm{e}} \approx 11.577 \frac{B}{10^{12}G} keV \tag{3}$$

(1) in (Potekhin, 2010)

It was believed that this would only result in emission features at first (e.g., Herold et al., 1982), but the resonant interaction behaviour of Landau electrons also results in absorption features in spectra of some X-ray sources (Fig.5). According to Heindl et al. (2004) objects with securely detected cyclotron features are, for example, Her X-1 at 41keV (Truemper et al., 1978), V 0332+53 at 24.9keV (Kreykenbohm et al., 2005) or Cep X-4 at 28keV (Mihara et al., 1991). Up to now, there are 16 sources with cyclotron features in their spectra (Caballero & Wilms, 2012). They are only way to measure the magnetic field of neutron stars directly at the moment (Caballero & Wilms, 2012).

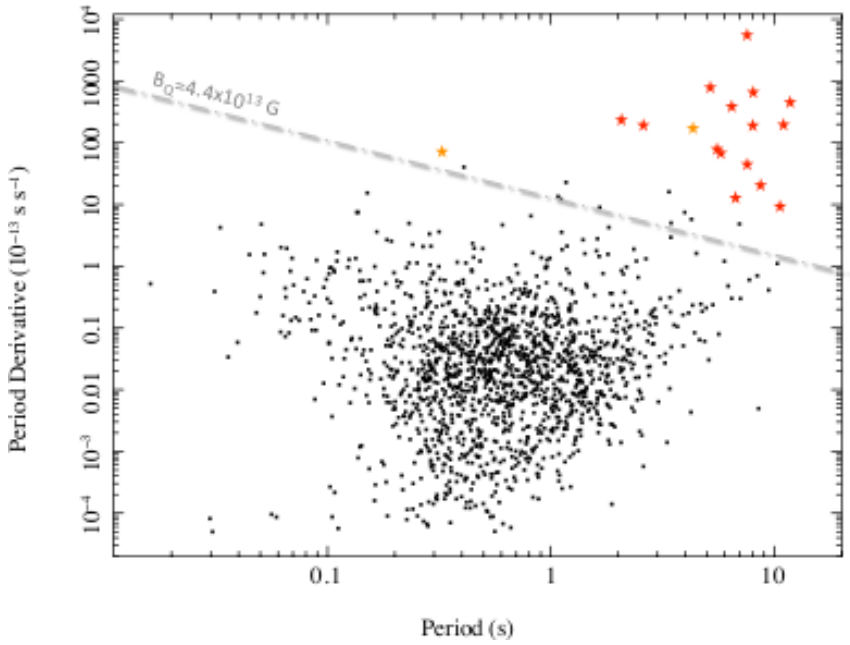

Figure 6: This plot is taken from (Hurley, 2010) and shows the spin period versus the spin-down of known isolated neutron stars. The stars in the top right are sources which could not be described by the behavior of neutron stars with the known probabilities.

1.3 Magnetars

These class of sources is historically called Soft Gamma Repeaters and Anomalous X-ray Pulsars. They are characterized by long periods $P \sim 2 - 11s$ and high spin-down rates $\dot{P} \sim 10^{-11} ss^{-1}$ (Fig.6,7). They show high quiescence X-ray emission from and stochastic bursts depending on the source from hard X-rays to soft γ-rays. The short stochastic bursts are believed to originate from cracks in crust in which energy is stored via toroidal magnetic tension and sporadically released (Perna & Pons, 2011). The authors compare the bursting behavior dependent of the age and birth magnetic magnetic field. Their results suggest that a magnetar shows SGR-like behavior in younger ages and AXP-like behavior in middle ages. The persistent X-ray emission and the high spin periods can be explained with the fact that changeing magnetic moments emit radiation like accelerated charges. The energy flux through a closed surface area equals the energy change in the surrounded volume. This is the base for the dipole breaking formula (Esposito et al., 2011):

$$B_s \approx 3.2 \cdot 10^{19} \sqrt{P\dot{P}G} \tag{4}$$

The most successful model to describe the behavior of this class of isolated neutron stars is the magnetar model (Thompson & Duncan, 1995). The term "Magnetar" is motivated by the fact that this subclass of neutron stars are assumed to have magnetic fields up to $B_s \approx 10^{15}$G. These high magnetic fields describe the spin-down rates with the energy loss by dipole radiation.

However the field at the surface is much too high to have resonant electron interaction, in the magnetosphere the emitted spectrum is changed by resonant photon-electron scattering (Rea et al., 2008). Because the mass of a proton is 3 orders of magnitude higher than

Figure 7: The table shows a quite up to date summary of currently known Magnetars and the candidate AXJ1844-0258. (Rea & Esposito, 2011)

Magnetars	RA (J2000)	Dec (J2000)	P (s)	$\dot{P}_{-12}$ (s/s)	B_{14} (G)	d[b] (kpc)
1E 2259+586[o]	23 01 08.29	+58 52 44.45	6.98	0.5	0.6	3.0
4U 0142+614[o]	01 46 22.44	+61 45 03.3	8.69	2.0	1.3	3.0
1RXS J1708−4009	17 08 46.87	-40 08 52.44	10.99	24*	4.7	3.8
1E 1048.1−5937[o]	10 50 07.14	-59 53 21.4	6.45	50*	4.4	2.7
1E 1841−045	18 41 19.34	-04 56 11.16	11.77	41	7.1	7.0
CXOU J0100−7211	01 00 43.14	-72 11 33.8	8.02	19	3.9	60
CXOU J1647−4552[o]	16 47 10.2	-45 52 16.9	10.61	0.9*	1.3	5.0
XTE J1810−197 [o]	18 09 51.08	-19 43 51.74	5.54	10*	1.6	2.5
1E 1547−5408[o]	15 50 54.11	-54 18 23.7	2.07	23 *	2.2	4.0
CXOU J1714−3810	17 14 05.74	-38 10 30.9	3.82	59	4.8	8.0
SGR 1806−20[o]	18 08 39.33	-20 24 39.94	7.55	10*	18	15
SGR 1900+14	19 07 14.33	+09 19 20.1	5.17	100*	6.5	15
SGR 0526−66	05 26 00.89	-66 04 36.3	8.05	65	7.3	55
SGR 1627−41 [o]	16 35 51.84	-47 35 23.3	2.59	19	2.2	11
SGR 0501+4516[o]	05 01 6.78	+45 16 34.0	5.76	6.8	2.0	5.0
SGR 0418+5729[o]	04 18 33.86	+57 32 22.91	9.08	<0.006	<0.075	2.0
SGR 1833−0832[o]	18 33 44.38	-08 31 07.71	7.56	4.0	1.8	10
PSR 1622−4950	16 22 44.8	-49 50 54.4	4.32	17	2.8	9.0
PSR J1846−0258	18 46 24.94	-02 58 30.1	0.32	7.1	0.5	6.0
AX J1844−0258[o,a]	18 44 54.68	-02 56 53.1	6.97	-	-	8.5

the mass of a electron and we are interested in magnetic fields with 3 orders of magnitude higher. The resonant proton cyclotron energy is given by:

$$\hbar\omega_{\rm p} = \hbar\omega_{\rm e}\frac{m_{\rm e}}{m_{\rm p}} \approx 6.305\frac{B}{10^{15}G}keV \tag{5}$$

Proton cyclotron resonance features are therefore expected in the soft X-rays. This would be a possibility to probe the magnetic field of a magnetar.

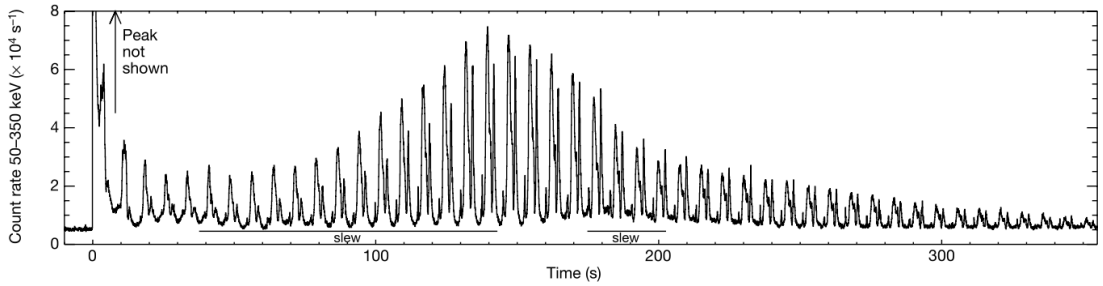

Figure 8: The flare was observed on December 27. 2004 with $2 \cdot 10^{46}$erg and reported in the paper (Palmer et al., 2005). The data was gathered with the "Burst Alert Telescope" onboard the "Swift" satellite.

1.4 Proton cyclotron absorption and the SGR 1806-20

There are only a few candidates for proton cyclotron features reported. One example is the Soft Gamma Repeater 1806-20. It is assumed to be centered in the the core of the Radio nebula G10.0-03, which is thought to be its supernova remnant. It is the most bursting active of all Soft Gamma Repeaters known today. The latest measurement of its period with $P = 7.6022 \pm 0.0007$s and the period derivative $\dot{P} = 75 \pm 4\,\mathrm{s\,s^{-1}}$ with data from Suzaku observations in the epoch MJD54189.0009 (Nakagawa et al., 2009). Ibrahim et al. (2003) analyzed phase resolved spectra of the SGR 1806-20 bursts from November 1996. The data was gathered with the Proportional Counter Array on board the Rossi X-ray Timing Explorer. They report an absorption feature at 5keV for a magnetic field of 10^{14}. In the the paper (Iwasawa et al., 1992), a feature around 5keV of the source AXP 1E1547.0-5408 is reported but due to lack of data not confirmed until today. The feature in the burst spectra of SGR 1806-20 also needs confirmation.

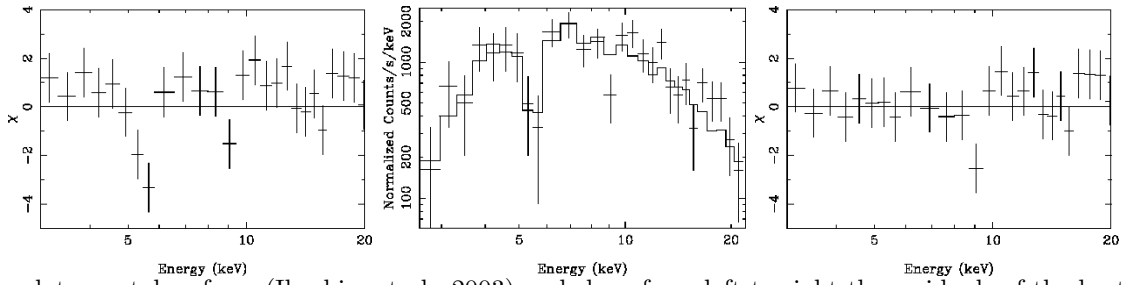

The plots are taken from (Ibrahim et al., 2003) and show from left to right the residuals of the best fit without an absorption Gaussian, a best fit pulse height spectrum with a sharp Gaussian at around $6keV$ and the residuals of this fit.

The radiative transfer in strongly magnetized accretion columns is the most influenced by resonant scattering (Daugherty & Ventura, 1978). Therefore, the quantum mechanical behavior of Landau protons in radiation will be re-investigated from a very basic level to first applications. The differential absorption cross sections of protons will be calculated to obtain the mean free path of a photon traveling through a medium with strongly magnetized protons.

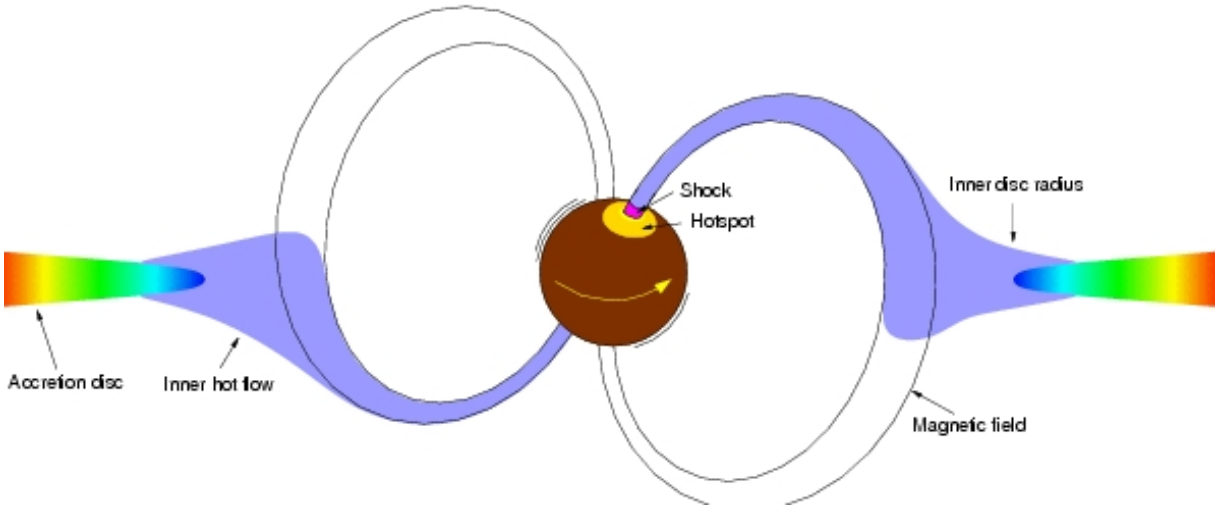

Figure 9: The picture is taken from [www.issibern.ch/teams/observephysics] and shows accretion streams to the poles of a neutron star that create radiation emitting hot spots. This scenario shows disk feed accretion.

2 Column formation

Concerning proton cyclotron features,the accreted matter is the main candidate as resonant cyclotron absorber. The region where resonant effects happen is called the "line forming region". The assumption of a homogeneous magnetic field along the z-axis in the line forming region is only valid if the accretion column can be approximated as a tube with a small ground surface, in other words, if the ground surface can be assumed a a flat surface. In this chapter, the orders of magnitude of values which constrain the geometry of an accretion column are evaluated to get a basic picture of the accretion column of a strongly magnetized neutron star. The values for Magnetars used in this chapter are:

$$M = 1.4 \cdot 10^{30}\text{kg} \qquad \dot{M} = 10^{12}\text{kg} \cdot \text{s}^{-1} \qquad B_s = 10^{11}\text{T} \qquad R_s = 1.2 \cdot 10^{4}\text{m}$$

The mass and the radius is obtained from (Meszaros, 1992, 1.2.15). To have a value to work with, the accretion rate is obtained from (Fürst et al., 2010) concerning the source Vela X-1.

2.1 Alfvén radius

The magnetic axis of accreting neutron stars, which we see as pulsating objects, is inclined to their rotation axis. However, the magnetic momentum here is consequently parallel to the rotation axis. The following approximation should therefore not be used if the axis between the magnetic and the rotation axis is not extraordinary high. To approximate the area on which the particles will hit the stellar surface, it is important to investigate the distance to the neutron star, where the magnetic fields get dominant, the Alfvén radius. This radius marks the border of the Magnetosphere. It can be investigated if the ram

pressure is compared to the magnetic fields energy density (Frank et al., 2002).

$$P_{\mathrm{ram}} = P_{\mathrm{B}} \tag{6}$$

In the simplest approximation, one can assume the neutron star as perfectly conducting sphere with a dipole-like external magnetic field (Meszaros, 1992).

$$B = \frac{\mu}{r^3} = B_s \frac{R_s^3}{r^3} \tag{7}$$

with the surface magnetic field B_s and the compact object radius R_s. Then the ram-pressure and the magnetic-field energy density are given by the quantities:

$$P_{\mathrm{ram}} = \rho_{(r)} \cdot (\dot{\vec{r}})^2 \tag{8}$$

and

$$P_B = \frac{B^2}{2\mu_0} \tag{9}$$

therefore (Eq. 2.1) becomes:

$$\rho_{(r)} \cdot (\dot{\vec{r}})^2 = \frac{B_{\mathrm{s}}^2 R_{\mathrm{s}}^6}{2\mu_0 r^6} \tag{10}$$

To evaluate the radius where the magnetic field energy, the situation is approximated. First, spheric symmetric inflow of matter is assumed. One should not forget that does not reflect reality because spherical symmetric super nova remnants which could feed the accretion are not expected. But with the assumption of radial spheric symmetric free fall the potential energy is completely transferred to radial kinetic energy the problem is highly simplified.

$$\dot{r}_{\mathrm{ff}} = \sqrt{\frac{2MG}{r}} \tag{11}$$

The mass is transferred homogeneously distributed spherically symmetric. So we get from the Continuity Equation:

$$\dot{M} = 4\pi \rho_{(r)} r^2 \dot{r} \tag{12}$$

This equation can be reformulated to:

$$\rho_{(r)} \dot{r} = \frac{\dot{M}}{4\pi r^2} \tag{13}$$

Therefore (Eq. 10) becomes:

$$\frac{\dot{M}}{4\pi r^2} \cdot \sqrt{\frac{2MG}{r}} = \frac{B_{\mathrm{s}}^2 R_{\mathrm{s}}^6}{2\mu_0 r^6} \tag{14}$$

which can be reformulated to:

$$r = \left(\frac{2\pi^2}{\mu_0^2 G}\right)^{\frac{1}{7}} \cdot \left(\frac{B_s^4 \cdot R_s^{12}}{\dot{M}^2 \cdot M}\right)^{\frac{1}{7}} \tag{15}$$

which leads to:

$$r = 2.1 \cdot 10^3 \cdot \left(\frac{B_s^4 \cdot R_s^{12}}{\dot{M}^2 \cdot M} \right)^{\frac{1}{7}} \tag{16}$$

This equation can be found in Frank et al. (2002). Applying the assumed values for Magnetars, one reads:

$$r_{\mathrm{A}} \approx 3 \cdot 10^8 m \tag{17}$$

To make sure the approximation of a small ground surface is still legal for higher matter flow concentrations one should look at the "worst case". Disks form if the accreted matter carries enough circular momentum, which it does if donated by a encircling binary companion. In spherical accretion, the matter in-fall is maximally spread. We expect a bigger column bottom for a smaller Alfv́en radius (Eq. 39). If we ignore the possibility of huge blobs of matter hitting the magnetosphere, a thin accretion disk is when the matter is concentrated the most for a given $\dot{M}$. A z independent $\rho_{(r)}$ in cylindrical coordinates allows to construct the continuity equation with an areal mass density:

$$\dot{M} = 2\pi \cdot r \cdot \dot{r}_{(r)} \cdot g_{(r)} \quad \Longleftrightarrow \quad \rho_{(r)} \cdot \dot{r}_{(r)} = \frac{\dot{M}}{2\pi \cdot r \cdot h_{(r)}} \tag{18}$$

With that we can rewrite the ram-pressure in a form that depends on the accretion rate $\dot{M}$.

$$P_{\mathrm{ram}} = \rho_{(r)} \cdot \dot{r}_{(r)} \dot{r}_{(r)} = \frac{\dot{M}}{2\pi \cdot r \cdot h_{(r)}} \cdot \dot{r}_{(r)} \tag{19}$$

The radial motion $\dot{r}_{(r)}$ is a bit harder to obtain:

$$r \partial_t \left(g_{(r)} \omega_{(r)} r^2 \right) + \partial_r \left(r^3 g_{(r)} \cdot \dot{r}_{(r)} \omega_{(r)} \right) = \frac{1}{2\pi} \partial_r G_{(r)} \tag{20}$$

With (Eq. 20) (see Frank et al., 2002, 5.4), which is derived from conservation equation of momentum, and the viscous torque(Frank et al., 2002, 4.27):

$$G_{(r)} = 2\pi r^3 g_{(r)} \cdot \xi_{(r)} \omega'_{(r)} \tag{21}$$

If a constant flow of matter and a constant density is assumed, one can set:

$$\partial_t \left(g_{(r)} \omega_{(r)} r^2 \right) = 0 \tag{22}$$

This simplifies (Eq. 20) to:

$$\partial_r \left(r^3 g_{(r)} \cdot \dot{r}_{(r)} \omega_{(r)} \right) = \partial_r \left(r^3 g_{(r)} \cdot \xi_{(r)} \omega'_{(r)} \right) \tag{23}$$

This equation can be reformulated to:

$$\partial_r \Bigg(r^3 g_{(r)} \Big(\dot{r}_{(r)} \omega_{(r)} - \xi (\partial_r \omega_{(r)}) \Big) \Bigg) = 0 \tag{24}$$

This equation for example is true if:

$$\Big(\dot{r}_{(r)} - \xi_{(r)} \partial_r \Big) \omega_{(r)} = 0 \Longleftrightarrow \dot{r}_{(r)} = \xi_{(r)} \frac{\partial_r \omega_{(r)}}{\omega_{(r)}} \tag{25}$$

If Keplerian circular motion is assumed in the disk, an expression for the radial velocity is found easy.

$$\omega_{(r)} = \sqrt{\frac{GM}{r^3}} \text{ so that } \partial_r \omega_{(r)} = \sqrt{\frac{GM}{r^3}} \cdot \left(\frac{-3}{2r}\right)$$

With the viscosity $\xi_{(r)}$, the radial speed $\dot{r}$ can be related to the radius r (Frank et al., 2002).

$$\dot{r}_{(r)} = -\left(\frac{3\xi_{(r)}}{2r}\right) \tag{26}$$

This approximation is only valid for $r \gg R_s$ because it ignores the interaction between surface and accreted matter. For strongly magnetized Neutron Stars, we expect an Alfvén radius with $r_A \gg R_s$. The equilibrium equation (Eq. 2.1) is only used in the disk, which can only exist at an $r > r_{\mathrm{A}}$. The area $r \approx r_A$ is ignored here. However, to investigate the column radius, this equation is a good guess for the order of magnitude of the radial velocity. A disk has different angular velocities at different radii. Because these rings interact with each other, the dynamics of a disk are highly non-trivial. The α-prescription taken from (Shakura & Sunyaev, 1973) helps to estimate $\xi_{(r)}$. With the sound-speed c_{s} and $\alpha \lesssim 1$, we can set:

$$\xi_{(r)} = \alpha \cdot c_{\mathrm{s}} \cdot h_{(r)} \tag{27}$$

$$P_{\mathrm{ram}} = \frac{3\dot{M}}{4\pi r^2 h_{(r)}} \cdot \xi_{(r)} = \frac{3\dot{M}\alpha c_{\mathrm{s}}}{4\pi r^2} \tag{28}$$

Bigger ram pressure P_{ram} leads to a smaller Alfvén radius r_{A}. We are interested in showing a "small" hit surface which gets smaller with larger r_{A}. because of that we can use the upper limit of P_{ram} to compare with magnetic pressure P_{B}. Highly supersonic movement is assumed:

$$\sqrt{\frac{2MG}{r}} > c_{\mathrm{s}} \tag{29}$$

With that, the ram pressure can be written as:

$$P_{\mathrm{ram}} = \frac{3\dot{M}\alpha c_{\mathrm{s}}}{4\pi r^2} < \frac{3\dot{M}c_{\mathrm{s}}}{4\pi r^2} < \frac{3\dot{M}}{4\pi r^2} \cdot \sqrt{\frac{2MG}{r}} \tag{30}$$

With () one can read:

$$\frac{B_{\mathrm{s}}^2 R_{\mathrm{s}}^6}{2\mu_0 r^6} < \frac{3\dot{M}}{4\pi r^2} \cdot \sqrt{\frac{2MG}{r}} \tag{31}$$

This leads to:

$$r > \left(\frac{2\pi^2}{9\mu^2 G}\right)^{\frac{1}{7}} \left(\frac{B_s^4 R_s^{12}}{\dot{M}^2 M}\right)^{\frac{1}{7}} \tag{32}$$

The difference to the spherical symmetric approximation is only $9^{-\frac{1}{7}} \approx 0.73$. AS lower limit for the Alfvén Radius one then can read:

$$r > 1.5 \cdot 10^8 m \tag{33}$$

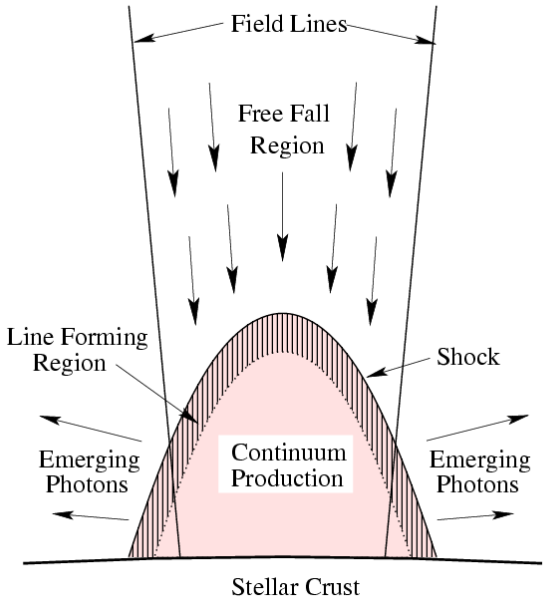

Figure 10: This picture shows a radiative shock in the accretion column and is taken from (Heindl et al., 2004)

2.2 Accretion column

The shape of accretion columns is not exactly known. There could be more than one, thin spaghetti like columns, wandering on the polar surface, or a hollow column (Meszaros, 1992). A hollow tube would be the imaginable as a high B field and $\dot{M}$ case compared to the shape of polar lights.
The surface emerging photons transfer upwards momentum to the plasma. This process depends on the temperature of the hot spot, which itself depends on $\dot{M}$ per unit surface. The luminosity of an object which it is powered via accretion can be related to its accretion rate via (Meszaros, 1992, 1.4.5):

$$L = \frac{GMM_{\odot}}{R} \tag{34}$$

According to (Duric, 2004, 9.4.2), fully ionized pure hydrogen is assumed as infalling matter and the sperical symmetric Thomson cross section σ_T is used to evaluate the critical luminosity, the Eddington luminosity. This is when the radiative pressure equals the ram pressure.

$$L_{Edd} = 1.3 \cdot 10^{38} \frac{M}{M_{\odot}} ergs^{-1} \tag{35}$$

In the vicinity of strong magnetic fields, the scattering behavior is not spherically symmetric. With the parallel and perpendicular cross sections $\sigma_{\parallel}$ and $\sigma_{\perp}$, the critical luminosity for magnetized sources reads (Basko & Sunyaev, 1976):

$$L_{\mathrm{crit}} = \frac{2.72 \cdot 10^{37} \sigma_{\mathrm{T}}}{\sqrt{\sigma_{\perp}\sigma_{\parallel}}} \left(\frac{A}{R_s}\right) \left(\frac{M_s}{M_{\odot}}\right) \mathrm{ergs}^{-1} \tag{36}$$

In sources with over-critical luminosity, a radiative shock is formed in the accretion column (Fig. 11). which raises the density of the line forming region. The formation of the shock flattens the emerging photon spectrum. In the shock photons are energized by Compton-scattering and emit X-ray spectra with a blackbody shape at high energies and a power law at high energies (Becker & Wolff, 2005), which broadens the spectrum to higher energies.
The spherical in-fall approximation and the thin disc approximation lead to a large Alfvén radius of $\approx 10^8$m. When a particle enters the magnetosphere at $r \approx r_A$, its trajectory can be viewed as completely constrained by the magnetic field. One could say, at the Alfvén radius the particle jumps onto a field line and follows it until it hits the surface. Because of dipole geometry, the angle to the magnetic axis in which a particle will hit the surface can be calculated simple (Frank et al., 2002).

$$r > C \cdot \sin^2 \theta \tag{37}$$

$C > 0$ is a constant identifying each field line. We put $r_\mathrm{A} = C$ and on the surface this equation becomes:

$$\frac{R_s}{r_\mathrm{A}} > \sin^2 \theta_s \quad \Longleftrightarrow \quad \theta_s < \arcsin \sqrt{\frac{R_s}{r_\mathrm{A}}} \tag{38}$$

The "Magnetar values" give us $\theta_s \approx 0.0058°$, which can be called "small". From that, one can conclude that the accretion flow will be concentrated on two small surfaces A on the polar caps with:

$$A = (R_s \cdot \sin(\theta_s))^2 \cdot \pi < \frac{R_s^3 \pi}{r_\mathrm{A}} \tag{39}$$

$$A < 10^4 m^2 \tag{40}$$

One can approximate that the inflow of mass onto the whole neutron star "system" equals the flow of mass onto the neutron stars surface at each moment. The "system" hereby includes everything that will hit the surface anytime in the future. This approximation is only valid if $\dot{M}$ does not change in time or if no kind of shock is assumed. This way, one can compare the continuity equation for complete surface with the continuity equation for the two surface pieces:

$$\dot{M} = 2A \cdot \rho_{(R_s)} \dot{r}_{(R_s)} \quad \Longleftrightarrow \quad \rho_{(R_s)} = \frac{\dot{M}}{2A\dot{r}_{(R_s)}} \tag{41}$$

With $A = \frac{R_s^3 \pi}{r_A}$, $\dot{r} = \sqrt{\frac{2MG}{R_s}}$, the approximated Alfvén radius from the chapter before ynd the "Magnetar values", one obtains as density at the bottom of the accretion column:

$$\rho_{(R_s)} = \frac{\dot{M}}{2^{\frac{3}{2}} \pi M^{\frac{1}{2}} G^{\frac{1}{2}} R_s^{\frac{5}{2}}} \cdot r_\mathrm{A} \approx 0.13 \frac{kg}{m^3} \tag{42}$$

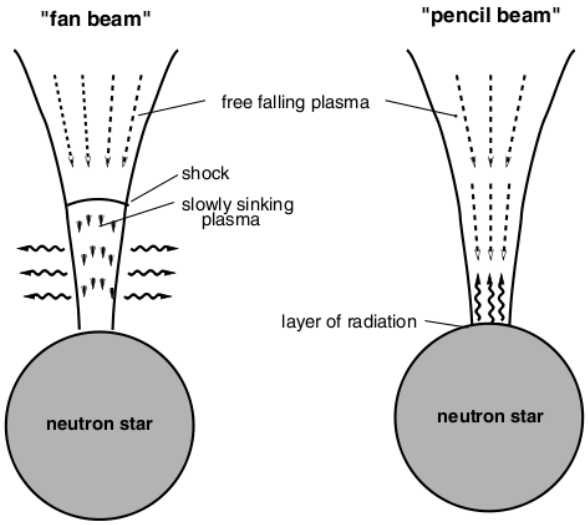

Figure 11: The pictures show fan beam with the formation of a shock and the pencil beam, which is without a shock (Schönherr et al., 2007).

2.3 Free fall speed at the surface

In the following the free fall speed will be evaluated. Because neutron stars are very heavy and very compact objects, one should keep in mind that the protons possibly will fall with $v \lesssim c$ at the z-axis near the surface. The object is quasi infinitely heavy, non-rotating and the metric in its rest-frame is therefore static. The movement of a relativistic particle can be calculated with the Geodesic equation (Landau & Lifschitz, a, 87.3):

$$\left(\frac{d}{d\tau}\right)^2 x^\zeta = \Gamma^\zeta_{\kappa\upsilon} \frac{dx^\kappa}{d\tau}\frac{dx^\upsilon}{d\tau} \tag{43}$$

Here, τ denotes the Eigenzeit which is connected to the coordinate time t via:

$$\frac{d}{d\tau} = \gamma \frac{d}{dt} \tag{44}$$

With:

$$\gamma = \sqrt{1 - \frac{v^2}{c^2}}^{-1} \tag{45}$$

The Christoffel symbols $\underline{\underline{\Gamma}}$, which contain derivatives of the metric, can be interpreted as the field if one interprets $\underline{\underline{g}}$ as kind of potential.

$$\Gamma^a_{bc} = g^{an}\left(\frac{\partial g_{nb}}{\partial x^c} + \frac{\partial g_{nc}}{\partial x^b} - \frac{\partial g_{bc}}{\partial x^n}\right) \tag{46}$$

The simplest case is when the test particle is falling directly towards the stellar surface. Then the situation is reduced to one dimension and we can constrain the movement of the test particle to the z-axis.

$$\underline{x} = \begin{pmatrix} ct \\ 0 \\ 0 \\ z \end{pmatrix} \qquad \left(\frac{d}{d\tau}\right)\underline{x} = \left(\frac{d}{d\tau}\right)\begin{pmatrix} ct \\ 0 \\ 0 \\ z \end{pmatrix} \tag{47}$$

A good way to describe a static gravitational field is the Schwarzschild metric:

$$\underline{\underline{g}} = \begin{bmatrix} -\left(1-\frac{2GM}{zc^2}\right) & 0 & 0 & 0 \\ 0 & 1 & 0 & 0 \\ 0 & 0 & 1 & 0 \\ 0 & 0 & 0 & \left(1-\frac{2GM}{zc^2}\right)^{-1} \end{bmatrix} \tag{48}$$

We clearly can see, the metric only depends on $z = x_3$ and all except the diagonal elements are 0. This simplifies the Christoffel symbols massively. In the following only the nonzero components are shown. The only interesting components of the Christoffel symbols are:

$$\Gamma^a_{00} = g^{an}\left(\frac{\partial g_{n0}}{\partial x^0} + \frac{\partial g_{n0}}{\partial x^0} - \frac{\partial g_{00}}{\partial x^n}\right) = -g^{a3}\frac{\partial g_{00}}{\partial x^3} \tag{49}$$

$$\Gamma^a_{33} = g^{an}\left(\frac{\partial g_{n3}}{\partial x^3} + \frac{\partial g_{n3}}{\partial x^3} - \frac{\partial g_{33}}{\partial x^n}\right) = g^{a3}\frac{\partial g_{33}}{\partial x^3} \tag{50}$$

$$\Gamma^a_{30} = \Gamma^a_{03} = g^{an}\left(\frac{\partial g_{n0}}{\partial x^3} + \frac{\partial g_{n3}}{\partial x^0} - \frac{\partial g_{03}}{\partial x^n}\right) = g^{a0}\frac{\partial g_{00}}{\partial x^3} \tag{51}$$

The metric is diagonal, as mentioned. therefore, the Christoffel symbols in the 3 equations above are always 0 except for the cases where "a" equals the neighboring index. This leads to the two differential equations:

$$\frac{d}{d\tau}\frac{dx^3}{d\tau} = \Gamma^3_{33}\frac{dx^3}{d\tau}\frac{dx^3}{d\tau} + \Gamma^3_{00}\frac{dx^0}{d\tau}\frac{dx^0}{d\tau} = g^{33}\frac{\partial g_{33}}{\partial x^3}\frac{dx^3}{d\tau}\frac{dx^3}{d\tau} - g^{33}\frac{\partial g_{00}}{\partial x^3}\frac{dx^0}{d\tau}\frac{dx^0}{d\tau} \tag{52}$$

$$\frac{d}{d\tau}\frac{dx^0}{d\tau} = \Gamma^0_{03}\frac{dx^0}{d\tau}\frac{dx^3}{d\tau} + \Gamma^0_{30}\frac{dx^3}{d\tau}\frac{dx^0}{d\tau} = 2g^{00}\frac{\partial g_{00}}{\partial x^3}\frac{dx^0}{d\tau}\frac{dx^3}{d\tau} \tag{53}$$

The second equation can simplified straight forward with the following equations:

$$\frac{d}{dt}\gamma = -\frac{2\dot{z}\ddot{z}}{c^2}\gamma^3 \quad \text{and} \quad \frac{\partial g_{00}}{\partial z} = -\frac{2GM}{z^2c^2} \tag{54}$$

$$\Longrightarrow$$

$$\ddot{z} = -\frac{2GM}{z^2}\left(1-\frac{2GM}{zc^2}\right)\left(1-\frac{\dot{z}^2}{c^2}\right) \tag{55}$$

This equation of motion can be integrated with a simple c code, using the gsl-integrator "gsl odeiv2". The mass and radius is obtained from the "magnetar values". One can find that different starting-heights in the order of magnitude of the Alfv́en radius lead to similar surface speed values of:

$$\dot{z} \approx \frac{2}{3}c \tag{56}$$

3 Landau Protons

In the following, the quantized behavior of protons in a strong magnetic field will be investigated. We expect quantized movement perpendicular to the magnetic field as in the case of landau electrons. On the other hand, the movement parallel to the field is not quantized. As mentioned, the formation of a shock is ignored and the matter is expected to be in free fall. Therefore, the z-momentum is dominated by gravitational acceleration and modified by temperature. If the matter is in thermal equilibrium, one can assume the z-momentum Boltzmann distributed in the rest frame.
To estimate the influence of relativistic effects, one can set the kinetic energy equal to the thermal and ground state energy.

$$(k_{\mathrm{B}}T)^2 + 2E_0(k_{\mathrm{B}}T) + E_0^2 = \left(\frac{m_{\mathrm{p}}c^2}{\sqrt{1-\frac{v^2}{c^2}}}\right)^2 - m_{\mathrm{p}}^2c^4 \tag{57}$$

Comparing the rest energy of a Proton $m_{\mathrm{p}}c^2$ is compared with the energy of the ground state E_0, one finds:

$$\frac{E_0}{m_{\mathrm{p}}c^2} = \frac{eB\hbar}{2m_{\mathrm{p}}^2c^3} \approx 3.4 \cdot 10^{-6} \ll 1 \tag{58}$$

Because of that the variation of the effective mass of the proton can also be ignored (Conte et al., 2004).

$$m_{\mathrm{p}}' = m_{\mathrm{p}}\sqrt{1 + n\frac{2eB\hbar}{m_{\mathrm{p}}^2c^3}} \approx m_{\mathrm{p}} \tag{59}$$

Compared to the rest mass, the kinetic energy stored in the x-y dimension is negligible, which is a valid approximation in the area of $10^{15}G$.

$$\left(\frac{k_{\mathrm{B}}T}{m_{\mathrm{p}}c^2}\right)^2 = \frac{1}{1-\frac{v^2}{c^2}} - 1 \iff \frac{v}{c} = \frac{1}{\sqrt{1+\left(\frac{m_{\mathrm{p}}c^2}{k_{\mathrm{B}}T}\right)^2}} \tag{60}$$

We can ignore the 1 in the denominator if it is small compared to the other addend.

$$\frac{m_{\mathrm{p}}c^2}{k_{\mathrm{B}}T} \approx \frac{11 \cdot 10^{12}}{T} \tag{61}$$

Because this quantity is for temperatures around 10^9K much larger than 1 we can approximate:

$$\frac{v}{c} \approx \frac{k_{\mathrm{B}}T}{m_{\mathrm{p}}c^2} \approx 10^{-4} \tag{62}$$

Now, if the accretion column has "only" a billion degrees, the Doppler effects caused by the thermal motion in z does not have to be taken into account. This allows us to calculate the interaction characteristics of Landau Protons with photons near the surface of strongly magnetized neutron stars, in non-relativistic Quantum Mechanics.

3.1 Hamilton operator

The behavior of a non-relativistic particle is given by the Schröedinger equation:

$$\widehat{H}\Psi = i\hbar\partial_t\Psi \tag{63}$$

With $\vec{A}$ as overlay of an external magnetic field and the field of electromagnetic waves, the Hamilton operator is given by (Landau & Lifschitz, b, 111.3):

$$\widehat{H} = \frac{1}{2m}\left(\widehat{p} - \frac{e}{c}\vec{A}\right)^2 \tag{64}$$

It makes sense to separate the Vector potential $\vec{A}$ in a static and a radiative part which is time dependent:

$$\frac{1}{2m}\left(\widehat{p} - \frac{e}{c}\vec{A}\right)^2 = \frac{1}{2m_\mathrm{p}}\left(\widehat{p} - \frac{e}{c}\left(\vec{A}_\mathrm{stat} + \vec{A}_\mathrm{rad}\right)\right)^2 \tag{65}$$

$$\vec{\nabla}\vec{A} = 0 \tag{66}$$

In Coulomb-gauge, which is given by the equation above, $\widehat{p}\vec{A} = 0 \iff \vec{k}\vec{A} = 0$ simplifies the operator to:

$$\widehat{H} = \frac{1}{2m_\mathrm{p}}\widehat{p}^2 + \frac{e^2}{2m_\mathrm{p}c^2}\vec{A}^2_\mathrm{stat} - \frac{e}{m_\mathrm{p}c}\vec{A}_\mathrm{rad}\widehat{p} - \frac{e}{m_\mathrm{p}c}\vec{A}_\mathrm{stat}\widehat{p} + \frac{e^2}{m_\mathrm{p}c^2}\vec{A}_\mathrm{rad}\vec{A}_\mathrm{stat} + \frac{e^2}{2m_\mathrm{p}c^2}\vec{A}^2_\mathrm{rad} \tag{67}$$

Comparing the static part of the Vector potential $\vec{A}_\mathrm{stat}$, which represents the magnetic field, with the radiative part $\vec{A}_\mathrm{rad}$, which represents a small perturbation in the form of a photon:

$$\vec{A}^2_\mathrm{stat} \gg \vec{A}^2_\mathrm{rad} \tag{68}$$

$$\vec{A}^2_\mathrm{stat} \gg \vec{A}_\mathrm{rad}\vec{A}_\mathrm{stat} \tag{69}$$

$$\Longrightarrow$$

$$\widehat{H} \approx \frac{1}{2m_\mathrm{p}}\widehat{p}^2 + \frac{e^2}{2m_\mathrm{p}c^2}\vec{A}^2_\mathrm{stat} - \frac{e}{m_\mathrm{p}c}\vec{A}_\mathrm{stat}\widehat{p} - \frac{e}{m_\mathrm{p}c}\vec{A}_\mathrm{rad}\widehat{p} \tag{70}$$

Perturbation theory allows to construct solutions, while ignoring parts of the Hamilton operator if small. Here, the only time dependent part is small. this allows us to construct stationary solutions.

$$\Psi_{(t)} = e^{-i\frac{E}{\hbar}t}\Psi \tag{71}$$

One now has to choose a representation for $\vec{A}$ which satisfies the Coulomb gauge constraint $\vec{\nabla}\vec{A} = 0$ and reproduces the magnetic field:

$$\vec{\nabla} \times \vec{A} = B\vec{e}_z \tag{72}$$

$$\vec{A}_\mathrm{stat} = \begin{pmatrix} -\frac{yB}{2} \\ \frac{xB}{2} \\ 0 \end{pmatrix} \tag{73}$$

Without the radiative part, the operator is time independent. With $\widehat{p} = -i\hbar\vec{\nabla}$, the unperturbed Hamiltonian is given by:

$$\widehat{H}_0 + \widehat{H}_z = \frac{1}{2m_\mathrm{p}}\left(\left(\frac{eB}{2c}\right)^2(x^2+y^2) - \hbar^2(\partial_x^2+\partial_y^2) + \frac{eB}{c}i\hbar(x\partial_y - y\partial_x)\right) - \frac{\hbar^2\partial_z^2}{2m_\mathrm{p}} \tag{74}$$

As mentioned before, we expect stationary solutions for protons perpendicular to B_z. If the Hamilton operator can be separated to addends (74), the solution can be constructed with factors. It makes therefore sense to separate the solutions in this way:

$$\varphi^n_{(\vec{x},t)} = e^{-i\frac{E_n}{\hbar}t}\nu^n_{(x,y)}\phi_{(z,t)} \tag{75}$$

3.2 Solutions perpendicular to B_z

In the following the Solutions $\nu^n_{(x,y)}$ are constructed. They have to satisfy the following differential equation:

$$\frac{1}{2m_\mathrm{p}}\left[\left(\frac{eB}{2c}\right)^2(x^2+y^2) - \hbar^2(\partial_x^2+\partial_y^2) + \frac{eB}{c}i\hbar(x\partial_y - y\partial_x)\right]\nu^n_{(x,y)} = E_n\nu^n_{(x,y)} \tag{76}$$

We expect a harmonic oscillator, e.g. Johnson & Lippmann (1949) and Landau & Lifschitz (b), which satisfies the following eigenvalue equation with the energies:

$$\widehat{H}_0\nu^n_{(x,y)} = E_n\nu^n_{(x,y)} \qquad\qquad E_n = \left(\frac{1}{2}+n\right)\hbar\frac{eB}{m_\mathrm{p}c} \tag{77}$$

A well known way to solve equations of the harmonic oscillator type is the ladder operator technique firstly shown by Dirac (1947).The ladder operators can be written as:

$$\hat{h}^+ = i\sqrt{\frac{\hbar c}{2eB}}\left[\left(\frac{eB}{2\hbar c}\right)(x-iy) - (\partial_x - i\partial_y)\right] \tag{78}$$

$$\hat{h}^- = -i\sqrt{\frac{\hbar c}{2eB}}\left[\left(\frac{eB}{2\hbar c}\right)(x+iy) + (\partial_x + i\partial_y)\right] \tag{79}$$

These "ladder"-operators have satisfy the following relations:

$$\hbar\frac{eB}{m_\mathrm{p}c}\hat{h}^-\hat{h}^+ = \widehat{H} + \frac{\hbar}{2}\frac{eB}{m_\mathrm{p}c} \qquad\qquad \hbar\frac{eB}{m_\mathrm{p}c}\hat{h}^+\hat{h}^- = \widehat{H} - \frac{\hbar}{2}\frac{eB}{m_\mathrm{p}c} \tag{80}$$

With these operators, one can push a state to a one step higher state, or reduce by one. The use of $\hat{h}^+$ and $\hat{h}^-$ as up and down operators is consistent with the expected energies.

$$\begin{aligned} E_{n\pm1}|\nu_x^{n\pm1}\rangle = \left(\frac{\hbar eB}{m_\mathrm{p}c}\hat{h}^\pm\hat{h}^\mp \pm \frac{\hbar eB}{2m_\mathrm{p}c}\right)\hat{h}^\pm|\nu_x^n\rangle = \hat{h}^\pm\left(\frac{\hbar eB}{m_\mathrm{p}c}\hat{h}^\mp\hat{h}^\pm \mp \frac{\hbar eB}{2m_\mathrm{p}c} \pm \frac{\hbar eB}{m_\mathrm{p}c}\right)|\nu_x^n\rangle = \\ \hat{h}^\pm\left(\widehat{H}_x \pm \frac{\hbar eB}{m_\mathrm{p}c}\right)|\nu_x^n\rangle = \left(E_n \pm \frac{\hbar eB}{m_\mathrm{p}c}\right)\hat{h}^\pm|\nu_x^n\rangle = \left(E_n \pm \frac{\hbar eB}{m_\mathrm{p}c}\right)|\nu_x^{n\pm1}\rangle \end{aligned} \tag{81}$$

QED

We expect that an application of the downwards operator to the ground state equals 0. therefore, we have a much easier differential equation to solve:

$$\left[\left(\frac{eB}{2\hbar c}\right)(x+iy) + (\partial_x + i\partial_y)\right]\nu^0_{(x,y)} = 0 \tag{82}$$

The ground-level energy can be calculated by replacing the Hamilton operator with an expression with $\hat{h}^-$ on the right hand side:

$$E_0|\nu^0\rangle = \widehat{H}_x|\nu^0\rangle = \left(\frac{\hbar eB}{m_\mathrm{p}c}\hat{h}^+\hat{h}^- + \frac{\hbar eB}{2m_\mathrm{p}c}\right)|\nu^0\rangle = \frac{\hbar eB}{2m_\mathrm{p}c}|\nu^0\rangle \tag{83}$$

A solution of (Eq. 82) can be found easy [.how...]. The constant can be obtained with the normalization constraint, which simply says that the probability of measuring the proton anywhere is 1, and a simple Gaussian integral. To keep a clear view, Mathematica scripts are quoted beneath the corresponding functions.

$$1 = \langle\nu^0|\nu^0\rangle = K^2\int\int e^{-\frac{eB}{2\hbar c}(x^2+y^2)}dxdy = K^2\frac{2\pi\hbar c}{eB} \tag{84}$$

$$\Longrightarrow \nu^0_{(x,y)} = \sqrt{\frac{eB}{2\pi\hbar c}}e^{-\frac{eB}{4\hbar c}(x^2+y^2)} \tag{85}$$

```
level[x_, y_, 0, 0] :=
  (charge B / (2 * Pi * ħ * c)) ^ (1 / 2) e^(- ((charge * B) / (4 * ħ * c)) * (x^2 + y^2));
```

This function stays a solution even if multiplied with multiples $(x - iy)$. This leads to a second quantum number with the ladder operators:

$$\hat{l}^+ = \sqrt{\frac{\hbar c}{2eB}}\left[\left(\frac{eB}{2\hbar c}\right)(x+iy) - (\partial_x + i\partial_y)\right] \tag{86}$$

$$\hat{l}^- = \sqrt{\frac{\hbar c}{2eB}}\left[\left(\frac{eB}{2\hbar c}\right)(x-iy) + (\partial_x - i\partial_y)\right] \tag{87}$$

The circular momentum ladder $\hat{l}^+$ operator leads to the following simple form for the ground states:

$$\nu^{0,l}_{(x,y)} = \left(\hat{l}^+\right)^l \nu^{0,0}_{(x,y)} = \sqrt{\frac{eB}{2\pi\hbar c}}\frac{1}{\sqrt{2^l l!}}\left(\frac{eB}{\hbar c}\right)^{\frac{l}{2}}(x+iy)^l e^{-\frac{eB}{4\hbar c}(x^2+y^2)} \tag{88}$$

```
level[x_, y_, 0, l_] :=
 (1 / (l!)) ^ (1 / 2) ((charge B / (2 ħ c)) ^ (1 / 2)) ^ l (x + ay y) ^ l level[x, y, 0, 0]
```

The higher levels, as stated before, can be found by applying the ladder operator $\hat{h}^+$ on the ground state $\nu^{0,l}$. The ladder operator $\hat{h}^+$ hereby reduces the circular momentum operator L_z by one. The Mathematica script reads:

```
level[x_, y_, n_, l_] := ay ((n - 1) ! / n!) ^ (1 / 2)
  ((ħ c) / (2 charge B)) ^ (1 / 2) ((charge B / (2 ħ c)) (x - ay y) level[x, y, n - 1, l + 1] -
    (D[level[x, y, n - 1, l + 1], x] - ay D[level[x, y, n - 1, l + 1], y]))
```

For practical reasons, special defined functions for the Landau levels are needed:

```
sol[x_, y_, n_, l_] := Expand[Expand[level[x, y, n, l]] /.
    Join[Table[ay^cplxa → If[Mod[cplxa, 2] == 0, If[Mod[(cplxa / 2), 2] == 0, 1, -1],
        If[Mod[cplxa, 4] == 3, -ay, ay]], {cplxa, 1, (4 + 4 * (n + l))}]] /. ay → i];
state[x_, y_, n_, l_] := Expand[Expand[level[x, y, n, l]] /.
   Join[Table[ay^cplxa → If[Mod[cplxa, 2] == 0, If[Mod[(cplxa / 2), 2] == 0, 1, -1],
       If[Mod[cplxa, 4] == 3, -ay, ay]], {cplxa, 1, (4 + 4 * (1 + n + l))}]]];
statecc[x_, y_, n_, l_] := Expand[Expand[level[x, y, n, l]] /.
    Join[Table[ay^cplxa → If[Mod[cplxa, 2] == 0, If[Mod[(cplxa / 2), 2] == 0, 1, -1],
        If[Mod[cplxa, 4] == 3, -ay, ay]], {cplxa, 1, (4 + 4 * (1 + n + l))}]] /. ay → -ay]
```

This solutions can be tested by applying the Hamilton operator on them. Because this calculation only consists of differentiations, one can let Mathematica do them to check if:

$$\widehat{H}\nu^{n,l}_{(x,y)} = \left(\frac{1}{2} + n\right)\hbar\frac{eB}{m_{\mathrm{p}}c}\nu^{n,l}_{(x,y)} \tag{89}$$

```
solution[n_, l_] := FullSimplify[
  (1 / (2 mass)) * (((charge * B) / (2 c))^2 * ((x^2 + y^2) sol[x, y, n, l]) -
      (ħ^2 (D[D[sol[x, y, n, l], x], x] + D[D[sol[x, y, n, l], y], y])) +
      (ħ * charge * B / c) * i * (x D[sol[x, y, n, l], y] - y D[sol[x, y, n, l], x])
    ) / sol[x, y, n, l]
 ]
```

One then can see that solution$[n, l]$ produces the correct energy Eigenvalue for all n and l. For example:

```
solution[1, 2]
```

$$\frac{3\,\mathrm{B}\,\mathrm{charge}\,\hbar}{2\,\mathrm{c}\,\mathrm{mass}}$$

Further, one can test if the quantum states are constructed with orthogonal solutions so that norm$[n, l] = 1$ for all n and l:

$$\langle\nu^{b,n}_{(x,y)}|\nu^{a,m}_{(x,y)}\rangle = \delta_{ab}\delta_{mn} \tag{90}$$

```
squa[x_, y_, n_, l_] := FullSimplify[
   Expand[(Expand[statecc[x, y, n, l]] /. ay → i) * (Expand[state[x, y, n, l]] /. ay → i)]] /
  e → e; norm[n_, l_] := Expand[squa[x, y, n, l]] /. Flatten[
   Table[e^(-(B charge (x^2+y^2))/(2 c ħ)) x^(2 p) y^(2 q) →
     (2 * Pi * (2 * q)! (2 * p)! (c * ħ / (B * charge))^(q + p + 1) / (2^(q + p) * q! * p!)),
     {p, 4 (n + l) + 2, 0, -1}, {q, 4 (n + l) + 2, 0, -1}]
   ]
```

For example:

```
norm[1, 3]
```

```
1
```

At the and it can be checked if the circular momentum operator $\widehat{L_z}$ produces the correct eigenvalues so that $\mathrm{rot}[x, y, n, l] = l$ for all n and l:

```
rot[x_, y_, n_, l_] :=
 FullSimplify[Expand[-ay (x * D[level[x, y, n, l], y] - y * D[level[x, y, n, l], x]) /.
      Join[Table[ay^cplxa -> If[Mod[cplxa, 2] == 0, If[Mod[(cplxa / 2), 2] == 0, 1, -1],
          If[Mod[cplxa, 4] == 3, -ay, ay]], {cplxa, 1, (n + l)}]] /. ay -> i] / sol[x, y, n, l]]
```

For example:

```
rot[x, y, 1, 4]
```

```
4
```

3.3 Solutions parallel to B_Z

The solution concerning the z dimension can be obtained by viewing the Landau proton as particle moving free in one direction.

$$-\frac{\hbar^2 \partial_z^2}{2m_\mathrm{p}} \mu_{(z,t)} = i\hbar \partial_t \mu_{(z,t)} \tag{91}$$

A constant momentum is represented by a plane wave.

$$\left(i\hbar\partial_t - \frac{\hbar^2 \partial_z^2}{2m_\mathrm{p}} \right) e^{i(k_z z - \omega t)} = 0 \tag{92}$$

This is a solution with the known k dependence of ω.

$$\omega_{(k_z)} = \frac{\hbar}{2m_\mathrm{p}} k_z^2 \tag{93}$$

The thermal motion is the cause for further line broadening. An energy distribution allows more photons to "hit" the resonance. One can construct $\mu_{(z,t)}$ as a wave package in one dimension, in other words, an infinite sum over wave functions, which are all solution to the reduced equation above. E.g. formula (2.18) in Merzbacher (1998):

$$\mu_{(z,t)} = \frac{1}{\sqrt{2\pi}} \int \widetilde{\mu}_{(k_z)} e^{i(k_z z - \omega t)} dk_z \tag{94}$$

We expect $\widetilde{\mu}_{(k_z)}$ to have a Gaussian shape. This is the case if the momenta are Boltzmann distributed in the z-dimension.

$$\widetilde{\mu}^*_{(k_z)} \widetilde{\mu}_{(k_z)} = \frac{\hbar}{\sqrt{2\pi m_\mathrm{p} k_B T}} e^{-\frac{\hbar^2}{2m_\mathrm{p} k_B T} k_z^2} \tag{95}$$

$$\widetilde{\mu}_{(k_z)} = \left(\frac{\hbar^2}{2\pi m_\mathrm{p} k_B T} \right)^{\frac{1}{4}} e^{-\frac{\hbar^2}{4m_\mathrm{p} k_B T} k_z^2} \tag{96}$$

Setting:

$$\widetilde{\mu}_{(k_z)} = \left(\frac{a}{\pi} \right)^{\frac{1}{4}} e^{-\frac{a}{2} k_z^2} \qquad \text{with} \qquad a = \frac{\hbar^2}{2m_\mathrm{p} k_B T} \tag{97}$$

One can rewrite equation (Eq. 96) and integrate over k_z from $-\infty$ to ∞ using (Eq. 156):

$$\mu_{(z,t)} = \left(\frac{a}{\pi}\right)^{\frac{1}{4}} \frac{1}{\sqrt{2\pi}} \int e^{-\frac{1}{2}\left(a+i\frac{\hbar t}{m_\mathrm{p}}\right)k_z^2} e^{izk_z} dk_z = \left(\frac{a}{\pi}\right)^{\frac{1}{4}} \frac{1}{\sqrt{a+i\frac{\hbar t}{m_\mathrm{p}}}} e^{-\frac{a-i\frac{\hbar t}{m_\mathrm{p}}}{2\left(a^2+\frac{\hbar^2 t^2}{m_\mathrm{p}^2}\right)}z^2} \tag{98}$$

3.4 Complete solution

The solutions are equivalent for example to the solutions Johnson & Lippmann (1949, 45). The difference is the charge and therefore an inverted phase factor.

$$\Psi^{n,l}_{(x,y)} = (-i)^n \frac{1}{\sqrt{l!n!2^n}} \sqrt{\frac{eB}{2\hbar c}}^{l+1} e^{\frac{eB}{4\hbar c}(x^2+y^2)+i\frac{p_z z}{\hbar}} (\partial_x + i\partial_y)^n \left[(x-iy)^l e^{-\frac{eB}{2\hbar c}(x^2+y^2)}\right] \tag{99}$$

The complete solutions for a Landau proton with a given momentum k in the z direction is given by:

$$\nu^{n,l}_{(x,y,z)} = \frac{1}{\sqrt{\pi l!n!}} \sqrt{\frac{eB}{2\hbar c}}^{l+1} (\hat{h}^+)^n (x+iy)^l e^{-\frac{eB}{4\hbar c}(x^2+y^2)} e^{i\frac{p_z z}{\hbar}} \tag{100}$$

With the Temperature T and with (Eq. 98), the Landau proton constructed as a wave packet in the z-dimension is given by:

$$\nu^{n,l}_{(x,y,z,T)} = \frac{1}{\sqrt{\pi l!n!}} \sqrt{\frac{eB}{2\hbar c}}^{l+1} (\hat{h}^+)^n (x+iy)^l e^{-\frac{eB}{4\hbar c}(x^2+y^2)} \mu_{(z,t)} \tag{101}$$

As mentioned, the ladder operator $\hat{h}^+$ reduces the angular momentum eigenvalue by 1. The solutions in the Mathematica code are named that way. One therefore has to keep in mind that in the code, "l" denotes the angular momentum eigenvalue directly.

4 Resonant absorption

We are interested in investigating resonant cyclotron absorption of radiation by protons in strong magnetic fields. However to get a complete picture, resonant emission has to be considered, in the following only the quantum mechanical absorption behavior of photons by protons will be investigated.

4.1 Absorption probabilities

Because the eigenstates of the proton are orthonormal, the scalar product of two of them, which describe the "jump"-probability if squared, is 0 for $a \neq b$.

$$\langle \nu^a | \nu^b \rangle = \delta_{ab} \tag{102}$$

The idea is to view a photon as small perturbation of a quantum state. This perturbation gives a probability, that the proton is jumping to an higher state, in other words, it absorbs the photon. The probability of transition from level a to b with an perturbation photon of $\vec{k}$ will occur in the time t is given by Fermi's golden rule (Merzbacher, 1998, 19.22):

$$P_{ab} = \left| \frac{i}{\hbar} \int_{-\frac{t}{2}}^{\frac{t}{2}} e^{i\frac{E_b - E_a}{\hbar}t} \langle \phi^b | \widehat{H}_{\mathrm{rad}} | \phi^a \rangle dt \right|^2 \tag{103}$$

We assume a magnetic field parallel to the z-axis. The emission and absorption characteristics are cylindrical symmetric and depend only on the angle to the magnetic field.

$$\vec{B} \parallel \vec{e}_z \tag{104}$$

It is therefore useful to limit the calculus to photons traveling on the x-axis.

$$k_y = 0 \tag{105}$$

The radiative part of the Hamilton operator can be obtained from (Eq.) in the chapter before.

$$\widehat{H}_{\mathrm{rad}} = -\frac{e}{m_{\mathrm{p}}c} \vec{A}_{\mathrm{rad}} \widehat{p} = -i \frac{e\hbar}{m_{\mathrm{p}}c} \vec{A}_{\mathrm{rad}} \vec{\nabla} \tag{106}$$

We construct the photon as a plane wave. The upper index denotes absorption and the lower index emission:

$$\vec{A}^{\pm}_{\mathrm{rad}} = a_{(\vec{k})} \vec{e}_{(\vec{k})} e^{\pm i(\vec{k}\vec{x} - \omega t)} \tag{107}$$

The probability of absorbing a photon which perturbates the quantum state from the time 0 to t' is:

$$P_{ab} = \frac{e^2 a^2_{(\vec{k})}}{m^2_{\mathrm{p}} c^2} \left| \int_{-\frac{t}{2}}^{\frac{t}{2}} e^{i\left(\frac{E_b - E_a}{\hbar} \mp \omega\right)t} \langle \phi^b | e^{\pm i\vec{k}\vec{x}} \vec{e}_{(\vec{k})} \vec{\nabla} | \phi^a \rangle dt \right|^2 \tag{108}$$

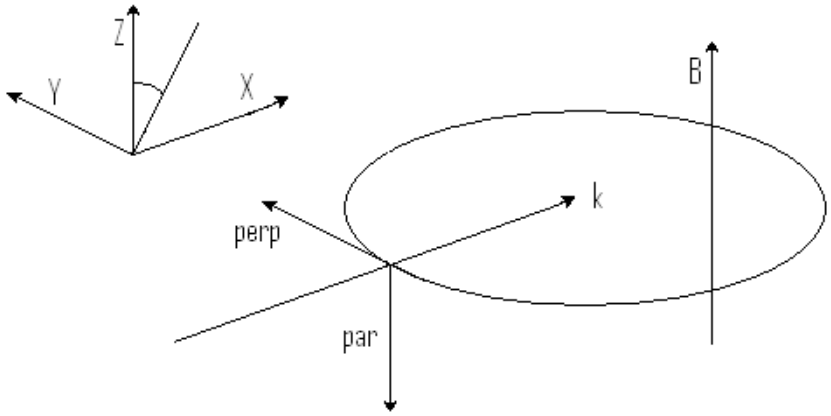

The polarisation of the photon can be constructed via a linear combination of vectors perpendicular to $\vec{k}$ with $a_\perp^2 + a_\parallel^2 = 1$. θ is the angle between $\vec{k}$ to z-axis.

$$\vec{e}(\vec{k}) = \left(a_{\perp(\vec{k})} \begin{pmatrix} 0 \\ 1 \\ 0 \end{pmatrix} + a_{\parallel(\vec{k})} \begin{pmatrix} \cos\theta \\ 0 \\ -\sin\theta \end{pmatrix} \right) \tag{109}$$

From the energy flux of the Poynting vector, one can derive the photon amplitude $a_{(\vec{k})}$. $N_{(\vec{k})}$ is the number of photons with $\hbar\omega$ Merzbacher (1998, 19.111):

$$N_{(\vec{k})}\hbar\omega = \frac{\omega^2}{2\pi c} a_{(\vec{k})}^2 \quad \Longleftrightarrow \quad a_{(\vec{k})}^2 = N_{(\vec{k})} \frac{2\pi\hbar c}{\omega} \tag{110}$$

A short form for the transition matrix element is defined:

$$P_{ab} = N_{(\vec{k})} \frac{2\pi\hbar e^2}{m_\mathrm{p}^2 c\omega} |M_{ab}|^2 \tag{111}$$

The parallel part does not depend on x or y and the perpendicular part depends only on z and t. It seems obvious to separate them. The perturbation matrix element then reads:

$$\begin{aligned} M_{ab} = \int e^{i\left(\frac{E_b - E_a}{\hbar} + \frac{\hbar k_b^2}{2m_\mathrm{p}} - \frac{\hbar k_a^2}{2m_\mathrm{p}} \mp \omega\right)t} \cdot \Big[& a_\parallel \cos\theta \langle \nu^b | e^{\pm i k_x x} \partial_x | \nu^a \rangle \langle \zeta | e^{\pm i k_z z} | \zeta \rangle + \\ & + a_\perp \langle \nu^b | e^{\pm i k_x x} \partial_y | \nu^a \rangle \langle \zeta | e^{\pm i k_z z} | \zeta \rangle - a_\parallel \sin\theta \langle \nu^b | e^{\pm i k_x x} | \nu^a \rangle \langle \zeta | e^{\pm i k_z z} \partial_z | \zeta \rangle \Big] dt \end{aligned} \tag{112}$$

4.2 Absorption rates

Imagine a plane wave propagating through a resonant absorbing medium of protons, perturbing the landau states. In the case of a photon, the time of perturbation is connected to the distance the photon has traveled. Therefore, the physically meaningful quantity to work with is the absorption rate. It is given by the transition probability per time from one state to a higher state.

$$\Gamma_{ab} = \frac{d}{dt} P_{ab} \tag{113}$$

The photon number $N_{(\vec{k})} = 1$ and the time of perturbation is t'. The probability to jump to a higher state absorbing a photon of a small momentum volume $d\vec{k}$ is given by:

$$P_{ab} = N_{(\vec{k})} \frac{2\pi\hbar e^2}{m_\mathrm{p}^2 c\omega} \left| \int_0^{t'} e^{i\left(\frac{E_b - E_a}{\hbar} - \omega\right)t} \langle \phi^b | e^{i\vec{k}\vec{x}} \vec{e}_{(\vec{k})} \vec{\nabla} | \phi^a \rangle dt \right|^2 \tag{114}$$

In thermal equilibrium one can expect that the kinetic energies of the Landau proton in z after the interaction is Boltzmann distributed. In the following, two different approaches are evaluated to find the absorption rate.

4.2.1 Transition from wave package to given z-momentum

In the first approach, the proton in the z-dimension is constructed as a plane wave before the interaction with a photon and has a fixed momentum after the interaction. Here, the z and t part of a absorption between a Landau proton and a perturbation photon will be evaluated:

$$\int_{-\frac{t}{2}}^{\frac{t}{2}} e^{i\left(\frac{E_b - E_a}{\hbar} - \omega\right)t} \langle \phi | e^{\pm i k_z z} | \phi \rangle dt = \int_{-\frac{t}{2}}^{\frac{t}{2}} e^{i\left(\frac{E_b - E_a}{\hbar} + \frac{\hbar k_b^2}{2m_\mathrm{p}} - \omega\right)t} \langle \zeta | e^{i k_z z} | \mu \rangle dt$$

$$= \left(\frac{a}{\pi}\right)^{\frac{1}{4}} \int_{-\frac{t}{2}}^{\frac{t}{2}} dt e^{i\left(\frac{E_b - E_a}{\hbar} + \frac{\hbar k_b^2}{2m_\mathrm{p}} - \omega\right)t} \frac{1}{\sqrt{a + i\frac{\hbar t}{m_\mathrm{p}}}} \int e^{+ik_\gamma z} e^{-\frac{1}{2\left(a + i\frac{\hbar t}{m_\mathrm{p}}\right)} z^2} dz =$$

$$= \sqrt{2\pi} \left(\frac{a}{\pi}\right)^{\frac{1}{4}} e^{-\frac{a}{2}k_\gamma^2} \int_{-\frac{t}{2}}^{\frac{t}{2}} e^{i\left(\frac{E_b - E_a}{\hbar} + \frac{\hbar k_b^2}{2m_\mathrm{p}} - \omega - \frac{\hbar k_\gamma^2}{2m_\mathrm{p}}\right)t} dt \tag{115}$$

$$\int_{-\frac{t}{2}}^{\frac{t}{2}} e^{i\left(\frac{E_b - E_a}{\hbar} - \omega\right)t} \langle \phi | e^{i k_z z} \partial_z | \phi \rangle dt = \int_{-\frac{t}{2}}^{\frac{t}{2}} e^{i\left(\frac{E_b - E_a}{\hbar} + \frac{\hbar k_b^2}{2m_\mathrm{p}} - \omega\right)t} \langle \zeta | e^{i k_z z} \partial_z | \mu \rangle dt$$

$$= \left(\frac{a}{\pi}\right)^{\frac{1}{4}} \int_{-\frac{t}{2}}^{\frac{t}{2}} dt e^{i\left(\frac{E_b - E_a}{\hbar} + \frac{\hbar k_b^2}{2m_\mathrm{p}} - \omega\right)t} \frac{1}{\sqrt{a + i\frac{\hbar t}{m_\mathrm{p}}}} \int e^{ik_\gamma z} \partial_z e^{-\frac{1}{2\left(a + i\frac{\hbar t}{m_\mathrm{p}}\right)} z^2} dz =$$

$$= -\left(\frac{a}{\pi}\right)^{\frac{1}{4}} \int_{-\frac{t}{2}}^{\frac{t}{2}} dt e^{i\left(\frac{E_b - E_a}{\hbar} + \frac{\hbar k_b^2}{2m_\mathrm{p}} - \omega\right)t} \frac{1}{\sqrt{a + i\frac{\hbar t}{m_\mathrm{p}}^3}} \int z e^{ik_\gamma z} e^{-\frac{1}{2\left(a + i\frac{\hbar t}{m_\mathrm{p}}\right)} z^2} dz =$$

$$= -ik_\gamma \sqrt{2\pi} \left(\frac{a}{\pi}\right)^{\frac{1}{4}} e^{-\frac{a}{2}k_\gamma^2} \int_{-\frac{t}{2}}^{\frac{t}{2}} e^{i\left(\frac{E_b - E_a}{\hbar} + \frac{\hbar k_b^2}{2m_\mathrm{p}} - \omega - i\frac{\hbar k_\gamma^2}{2m_\mathrm{p}}\right)t} dt \tag{116}$$

From the time integral, one simply obtains a "Sinc". Because this function is going to be integrated over broad k_b, one can replace the Sinc with a delta function according to (Eq. 142):

$$\int_{-\frac{t}{2}}^{\frac{t}{2}} e^{i\left(\frac{E_b-E_a}{\hbar}+\frac{\hbar k_b^2}{2m_\mathrm{p}}-\omega-\frac{\hbar k_\gamma^2}{2m_\mathrm{p}}\right)t}dt = \left(\frac{e^{i\left(\frac{E_b-E_a}{\hbar}+\frac{\hbar k_b^2}{2m_\mathrm{p}}-\omega-\frac{\hbar k_\gamma^2}{2m_\mathrm{p}}\right)t}-e^{-i\left(\frac{E_b-E_a}{\hbar}+\frac{\hbar k_b^2}{2m_\mathrm{p}}-\omega-\frac{\hbar k_\gamma^2}{2m_\mathrm{p}}\right)t}}{\frac{2}{2}i\left(\frac{E_b-E_a}{\hbar}+\frac{\hbar k_b^2}{2m_\mathrm{p}}-\omega-\frac{\hbar k_\gamma^2}{2m_\mathrm{p}}\right)}\right)^2 =$$

$$= \left(\frac{\sin\left(\frac{\frac{E_b-E_a}{\hbar}+\frac{\hbar k_b^2}{2m_\mathrm{p}}-\omega-\frac{\hbar k_\gamma^2}{2m_\mathrm{p}}}{2}t\right)}{\left(\frac{\frac{E_b-E_a}{\hbar}+\frac{\hbar k_b^2}{2m_\mathrm{p}}-\omega-\frac{\hbar k_\gamma^2}{2m_\mathrm{p}}}{2}\right)}\right)^2 \approx 2\pi t\delta\left(\frac{E_b-E_a}{\hbar}+\frac{\hbar k_b^2}{2m_\mathrm{p}}-\omega-\frac{\hbar k_\gamma^2}{2m_\mathrm{p}}\right) \quad (117)$$

The last part in the delta function represents a measurement of the the kinetic energy of the Landau proton in z before the interaction. This is a consequence of momentum conservation. With $k_\gamma = k_z$, the absorption probability from level a to b per time with the absorption of a single photon, therefore $N_{(\vec{k})} = 1$ and a given $\vec{k}$ is:

$$\Gamma_{ab} = \frac{2\pi\hbar e^2}{m_\mathrm{p}^2 c\omega}\frac{d}{dt}|M_{ba}|^2 = (2\pi)^3\left(\frac{a}{\pi}\right)^{\frac{1}{2}}\frac{\hbar e^2}{m_\mathrm{p}^2 c\omega}\delta_{\left(\frac{E_b-E_a}{\hbar}+\frac{\hbar k_b^2}{2m_\mathrm{p}}\mp\omega-\frac{\hbar k_z^2}{2m_\mathrm{p}}\right)}e^{-ak_z^2}\cdot$$
$$\cdot\left|a_\parallel\cos\theta\langle\nu^b|e^{-ik_x x}\partial_x|\nu^a\rangle + a_\perp\langle\nu^b|e^{-ik_x x}\partial_y|\nu^a\rangle - ia_\parallel\sin\theta k_z\langle\nu^b|e^{-ik_x x}|\nu^a\rangle\right|^2 \quad (118)$$

In the following $\rho_{(k_z)}$ is reformulated to $\rho_{(T_b)}$ with a substitution.

$$1 = \int_0^\infty \frac{2\hbar}{\sqrt{2\pi m_\mathrm{p} k_\mathrm{B} T}}e^{-\frac{\hbar^2 k_b^2}{2m_\mathrm{p}k_\mathrm{B}T}}dk_b =$$
$$= \left|T_b = \frac{\hbar^2 k_b^2}{2m_\mathrm{p}}; dk_b = dT_b\frac{1}{\sqrt{T_b}}\sqrt{\frac{m}{2}}\frac{1}{\hbar}\right| =$$
$$= \int_0^\infty \frac{2}{\sqrt{\pi k_\mathrm{B}T}}\frac{1}{\sqrt{T_b}}e^{-\frac{T_b}{k_\mathrm{B}T}}dT_b \quad (119)$$

Due to the delta distribution, the kinetic energy integration can be obtained easy.

$$\int \rho_{(T_b)}\delta_{\left(\frac{E_b-E_a}{\hbar}+\frac{\hbar k_b^2}{2m_\mathrm{p}}-\omega-\frac{\hbar k_z^2}{2m_\mathrm{p}}\right)}dT_b = \hbar\int\rho_{(T_b)}\delta_{\left(T_b+E_b-E_a-\hbar\omega-\frac{\hbar^2k_z^2}{2m_\mathrm{p}}\right)}dT_b =$$
$$= \hbar\rho_{\left(-E_b+E_a+\hbar\omega+\frac{\hbar^2k_z^2}{2m_\mathrm{p}}\right)} = \frac{2\hbar}{\sqrt{\pi k_\mathrm{B}T}}\frac{e^{-\frac{\left|-E_b+E_a+\hbar\omega+\frac{\hbar^2k_z^2}{2m_\mathrm{p}}\right|}{k_\mathrm{B}T}}}{\sqrt{\left|-E_b+E_a+\hbar\omega+\frac{\hbar^2k_z^2}{2m_\mathrm{p}}\right|}} \quad (120)$$

The z-axis, the absorption probability per time, per ω, per θ, per φ reads:

$$\frac{d\Gamma_{ab}}{d\omega d\theta d\varphi dt} = \frac{8\pi^2\hbar^3 e^2}{\sqrt{2m_{\rm p}}k_{\rm B}Tm_{\rm p}^2 c\omega} \frac{e^{-\frac{\left|-E_b+E_a+\hbar\omega+\frac{\hbar^2k_z^2}{2m_{\rm p}}\right|}{k_{\rm B}T}} e^{-\frac{\hbar^2\omega^2\cos\theta^2}{2m_{\rm p}c^2k_{\rm B}T}}}{\sqrt{\left|-E_b+E_a+\hbar\omega+\frac{\hbar^2k_z^2}{2m_{\rm p}}\right|}} \frac{\omega^2}{c^3}\sin\theta\cdot$$

$$\cdot\left|a_\parallel\cos\theta\langle\nu^b|e^{ik_xx}\partial_x|\nu^a\rangle + a_\perp\langle\nu^b|e^{ik_xx}\partial_y|\nu^a\rangle + ia_\parallel\frac{\omega}{c}\sin\theta\cos\theta\langle\nu^b|e^{ik_xx}|\nu^a\rangle\right|^2 \quad (121)$$

$$m_{ab} = \left[a_\parallel\cos\theta\langle\nu^b|e^{ik_xx}\partial_x|\nu^a\rangle + a_\perp\langle\nu^b|e^{ik_xx}\partial_y|\nu^a\rangle + ia_\parallel\frac{\omega}{c}\sin\theta\cos\theta\langle\nu^b|e^{ik_xx}|\nu^a\rangle\right] \quad (122)$$

With (Eq. 122), the Mathematica code to calculate m_{ab} is:

```
mabs[nin_, nout_, lin_, lout_, θ_, ω_, par_, perp_] := Expand[
     Cos[θ] * statecc[x, y, nout, lout] *
       e^(+ay * (ω / c) * Sin[θ] * x) * D[state[x, y, nin, lin], x] * (par) +
      statecc[x, y, nout, lout] * e^(+ay * (ω / c) * Sin[θ] * x) *
       D[state[x, y, nin, lin], y] * (perp) +
      ay * (ω / c) * Cos[θ] * Sin[θ] * statecc[x, y, nout, lout] *
       state[x, y, nin, lin] * e^(+ay * (ω / c) * Sin[θ] * x) * (par)
    ] /.
    Join[
     Table[e^-(B charge (x^2+y^2))/(2 c ħ) + (ay ω x Sin[θ])/c y^l → 0,
      {l, (3 * (nin + nout + lin + lout) + 1 + Mod[(nin + nout + lin + lout), 2]), 1, -2}]
     ,
     Flatten[
      Table[e^-(B charge (x^2+y^2))/(2 c ħ) + (ay ω x Sin[θ])/c x^p y^2 q →
        ((2 * Pi * c * ħ / (B charge))^(1 / 2) * (2 * q)! (c * ħ)^q / ((B charge)^q * 2^q * q!)) *
         e^(-ω^2 * Sin[θ]^2 * ħ / (2 c * B charge)) * p! * (+ay ω * ħ * Sin[θ] / (B charge))^p *
         Sum[(1 / (j! * (p - 2 * j)!)) * (B charge c / (-2 * ħ * ω^2 * Sin[θ]^2))^j,
          {j, 0, ((p - Mod[p, 2]) / 2)}],
       {p, 4 * (4 + nin + nout + lin + lout), 0, -1}, {q, 4 * (4 + nin + nout + lin + lout), 0, -1}]
     ]
    ] /. Join[Table[ay^cplxa → If[Mod[cplxa, 2] == 0, If[Mod[(cplxa / 2), 2] == 0, 1, -1],
       If[Mod[cplxa, 4] == 3, -ay, ay]], {cplxa, 1, 4 + 4 * (nin + nout)}]];
```

The code to evaluate the square of the matrix element with the time part is:

```
mabssq[nin_, nout_, lin_, lout_, θ_, gen_, par_, perp_] :=
 Expand[(8 Pi^2 ħ^3 charge / ((2 mass)^(1 / 2) boltzmann T mass gen B))
   (e^-((B charge (-nout+gen+nin) ħ / (boltzmann c mass T) + B^2 charge^2 gen^2 ħ^2 Cos[θ]^2 / (2 boltzmann mass^3 c^4 T))^2)^(1/2)
   e^-(B^2 charge^2 gen^2 ħ^2 Cos[θ]^2 / (2 boltzmann mass^3 c^4 T)) /
   Sqrt[(Sqrt[((gen * charge * B / (mass * c)) ħ Cos[θ]) / (Sqrt[2] c Sqrt[mass])]^2 +
       1/(c mass) B charge ((-nout + gen + nin)^2)^(1 / 2) ħ)^2]
   ((gen * charge * B / (mass * c))^2 / (c^3)) Sin[θ]
   (Expand[mabs[nin, nout, lin, lout, θ, (gen * charge * B / (mass * c)), par, perp]] /. ay → -i) *
   (Expand[mabs[nin, nout, lin, lout, θ, (gen * charge * B / (mass * c)), par, perp]] /. ay → i)]
```

A photon is carrying spin ± 1. This means, if a Landau proton interacts with a photon by absorbing or emitting, circular momentum must also be transferred.

$$\Delta L_z = \pm 1 \tag{123}$$

Transitions with a spin switch which also represent a change of circular momentum are ignored in this work. As expected, the forbidden transition matrix elements are 0 which can be shown with the following Mathematica script:

```
mabssqint[nin_, nout_, lin_, lout_, θ_, gen_] :=
 Integrate[Expand[mabssq[nin, nout, lin, lout, θ, gen, Cos[var], Sin[var]]], {var, 0, π / 2}]
```

For example:

```
mabssqint[0, 2, 0, 0, Pi / 2, gen]
```

```
0
```

To evaluate the absorption rate, one has to sum over all possible end states:

```
mabssqintsum[nend_, θ_, gen_] := Sum[mabssqint[0, nout, 0, 1, θ, gen], {nout, 1, nend}]
```

The following plots show the angle dependent absorption rate of a resonant photon. All circular momentum quantum number transitions are from 0 to 1 and show the probability per time that resonant photon, in form of a plane wave, gets absorbed with the denoted level jump

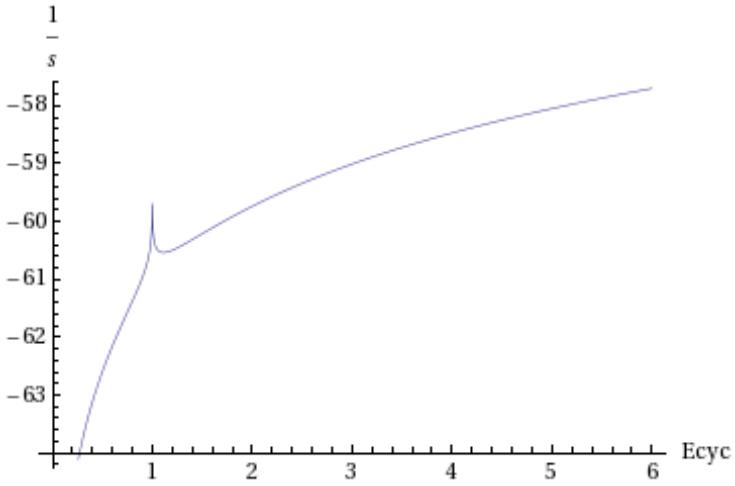

Figure 12: The plot shows the absorption rate in logarithmic scale. Interesting is that the first resonance dominates the complete interaction.

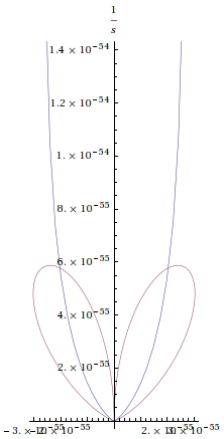

From Landau level 0 to 1

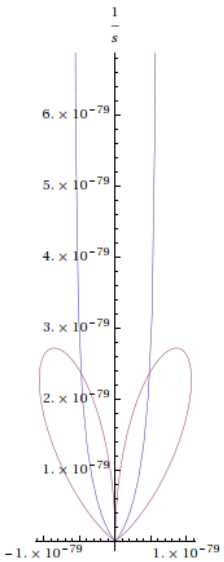

From Landau level 0 to 2

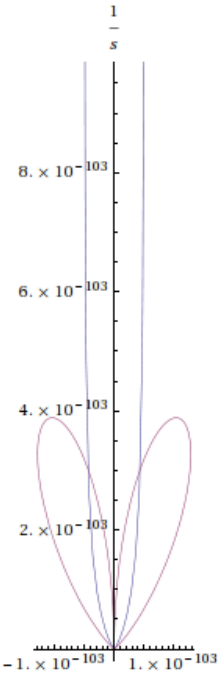

From Landau level 0 to 3

4.2.2 Transition between wave packages

In the second approach, the proton momentum in the z dimension will be constructed as wave package before and after it has absorbed a photon. This means the photon is only pushing the proton to a higher Landau level. The construction of $\mu_{(z,t)}$ as a wave package has the advantage that integrations over the whole space are clean to do. In the following interaction from a Landau proton in the ground state to a higher state, from a wave packet to the same wave packet will be assumed.

$$\langle\mu|e^{ik_\gamma z}|\mu\rangle = \left(\frac{a}{\pi}\right)^{\frac{1}{2}} \frac{1}{\sqrt{a^2+\frac{\hbar^2t^2}{m_\mathrm{p}^2}}} \int e^{-\frac{a}{a^2+\frac{\hbar^2t^2}{m_\mathrm{p}^2}}z^2} e^{ik_\gamma z} dz = e^{-\frac{a}{4}k_\gamma^2} e^{-\frac{\hbar^2k_\gamma^2}{4am_\mathrm{p}^2}t^2} \tag{124}$$

$$\begin{aligned}\langle\mu|e^{ik_\gamma z}\partial_z|\mu\rangle &= -\left(\frac{a}{\pi}\right)^{\frac{1}{2}} \frac{1}{\sqrt{a-i\frac{\hbar t}{m_\mathrm{p}}}\sqrt{a+i\frac{\hbar t}{m_\mathrm{p}}}^3} \int z e^{-\frac{a}{\left(a^2+\frac{\hbar^2t^2}{m_\mathrm{p}^2}\right)}z^2} e^{ik_\gamma z} dz = \\ &= -\frac{1}{\sqrt{a^2+\frac{\hbar^2t^2}{m_\mathrm{p}^2}}\left(a+i\frac{\hbar t}{m_\mathrm{p}}\right)} \sqrt{a^2+\frac{\hbar^2t^2}{m_\mathrm{p}^2}} \frac{ik_\gamma\left(a^2+\frac{\hbar^2t^2}{m_\mathrm{p}^2}\right)}{2a} e^{-\frac{a}{4}k_\gamma^2} e^{-\frac{\hbar^2k_\gamma^2}{4am_\mathrm{p}^2}t^2} = \\ &= -k_\gamma \frac{1}{a}\left(ia+\frac{\hbar t}{m_\mathrm{p}}\right) e^{-\frac{a}{4}k_\gamma^2} e^{-\frac{\hbar^2k_\gamma^2}{4am_\mathrm{p}^2}t^2}\end{aligned} \tag{125}$$

Here, we are only interested if a transition to a higher level by destroying a photon with given $\vec{k}$ happens or not. We therefore allow the photon to interact infinite time, which leads to an infinite time integration. With (Eq. 97), one then can obtain:

$$\int e^{i\left(\frac{E_b-E_a}{\hbar}-\omega\right)t}\langle\mu|e^{ik_\gamma z}|\mu\rangle dt = \sqrt{\frac{\pi m_\mathrm{p}}{k_BT}}\frac{1}{k_\gamma} e^{-\frac{\hbar^2}{8m_\mathrm{p}k_BT}k_\gamma^2} e^{-\frac{m_\mathrm{p}}{2k_BTk_\gamma^2}\left(\frac{E_b-E_a}{\hbar}-\omega\right)^2} \tag{126}$$

$$\begin{aligned}&\int e^{i\left(\frac{E_b-E_a}{\hbar}-\omega\right)t}\langle\mu|e^{ik_\gamma z}\partial_z|\mu\rangle dt = \\ &= -i\left(\frac{k_\gamma}{2}+\frac{m_\mathrm{p}}{\hbar k_\gamma}\left(\frac{E_b-E_a}{\hbar}\mp\omega\right)\right)\sqrt{\frac{\pi m_\mathrm{p}}{k_BT}}\frac{1}{k_\gamma} e^{-\frac{\hbar^2}{8m_\mathrm{p}k_BT}k_\gamma^2} e^{-\frac{m_\mathrm{p}}{2k_BTk_\gamma^2}\left(\frac{E_b-E_a}{\hbar}-\omega\right)^2}\end{aligned} \tag{127}$$

with:

$$\frac{E_b-E_a}{\hbar} = \frac{eB}{m_\mathrm{p}c}(b-a) \tag{128}$$

and:

$$k_\gamma = \frac{\omega}{c}\cos\theta \tag{129}$$

And the equations (Eq. 126) and (Eq. 127) putted in the matrix elements, one can read:

$$M_{ab} = \sqrt{\frac{\pi m_{\mathrm{p}}}{k_B T}} \frac{c}{\omega \cos\theta} e^{-\frac{\hbar^2}{8 m_{\mathrm{p}} c^2 k_B T} \omega^2 \cos\theta^2} e^{-\frac{m_{\mathrm{p}} c^2}{2 k_B T \omega^2 \cos\theta^2} \left(\frac{eB}{m_{\mathrm{p}} c}(b-a)-\omega\right)^2} \cdot$$
$$\left[a_{\parallel} \cos\theta \langle \nu^b | e^{i k_x x} \partial_x | \nu^a \rangle + a_{\perp} \langle \nu^b | e^{i k_x x} \partial_y | \nu^a \rangle + \right.$$
$$\left. + i \left(\frac{\omega \cos\theta}{2c} + \frac{m_{\mathrm{p}} c}{\hbar \omega \cos\theta} \left(\frac{eB}{m_{\mathrm{p}} c}(b-a) - \omega \right) \right) a_{\parallel} \sin\theta \langle \nu^b | e^{i k_x x} | \nu^a \rangle \right] \quad (130)$$

In the end, the probability rate of absorbing a photon with a given θ and ω while a level jump from state a to b reads:

$$\frac{dP_{ab(\omega,\theta)}}{d\theta d\omega d\varphi dt} = \frac{2e^2\pi^2}{m_{\mathrm{p}} k_B T} \frac{\hbar c}{\omega^3 \cos\theta^2} e^{-\frac{\hbar^2}{4 m_{\mathrm{p}} c^2 k_B T} \omega^2 \cos\theta^2} e^{-\frac{m_{\mathrm{p}} c^2}{k_B T \omega^2 \cos\theta^2} \left(\frac{eB}{m_{\mathrm{p}} c}(b-a)-\omega\right)^2} \frac{\omega^2}{c^3} \sin\theta \cdot$$
$$\cdot \left| a_{\parallel} \cos\theta \langle \nu^b | e^{i k_x x} \partial_x | \nu^a \rangle + a_{\perp} \langle \nu^b | e^{i k_x x} \partial_y | \nu^a \rangle + \right.$$
$$\left. + i \left(\frac{\omega \cos\theta}{2c} + \frac{m_{\mathrm{p}} c}{\hbar \omega \cos\theta} \left(\frac{eB}{m_{\mathrm{p}} c}(b-a) - \omega \right) \right) a_{\parallel} \sin\theta \langle \nu^b | e^{i k_x x} | \nu^a \rangle \right|^2 \quad (131)$$

The Mathematica code to calculate the matrix elements for transitions from wave package to wave package is:

```
mabs[nin_, nout_, lin_, lout_, θ_, ω_, par_, perp_] := Expand[
    Cos[θ] * statecc[x, y, nout, lout] *
      e^(+ay * (ω / c) * Sin[θ] * x) * D[state[x, y, nin, lin], x] * (par) +
     statecc[x, y, nout, lout] * e^(+ay * (ω / c) * Sin[θ] * x) *
      D[state[x, y, nin, lin], y] * (perp) +
     ay * ((ω Cos[θ] / (2 c)) + (mass c / (ħ ω Cos[θ])) * ((charge B / (mass c)) * (nout - nin) - ω)) *
      Sin[θ] * state[x, y, nout, lout] * statecc[x, y, nin, lin] *
      e^(+ay * (ω / c) * Sin[θ] * x) * (par)
   ] /.
   Join[
    Table[e^-(B charge (x^2+y^2))/(2 c ħ) + (ay ω x Sin[θ])/c y^l → 0,
     {l, (3 * (nin + nout + lin + lout) + 1 + Mod[(nin + nout + lin + lout), 2]), 1, -2}]
    ,
    Flatten[
     Table[e^-(B charge (x^2+y^2))/(2 c ħ) + (ay ω x Sin[θ])/c x^p y^(2 q) →
       ((2 * Pi * c * ħ / (B charge))^(1 / 2) * (2 * q)! (c * ħ)^q / ((B charge)^q * 2^q * q!)) *
        e^(-ω^2 * Sin[θ]^2 * ħ / (2 c * B charge)) * p! * (+ay ω * ħ * Sin[θ] / (B charge))^p *
        Sum[(1 / (j! * (p - 2 * j)!)) * (B charge c / (-2 * ħ * ω^2 * Sin[θ]^2))^j,
         {j, 0, ((p - Mod[p, 2]) / 2)}],
      {p, 4 * (4 + nin + nout + lin + lout), 0, -1}, {q, 4 * (4 + nin + nout + lin + lout), 0, -1}]
    ]
   ] /. Join[Table[ay^cplxa → If[Mod[cplxa, 2] == 0, If[Mod[(cplxa / 2), 2] == 0, 1, -1],
      If[Mod[cplxa, 4] == 3, -ay, ay]], {cplxa, 1, 4 + 4 * (nin + nout)}]]
```

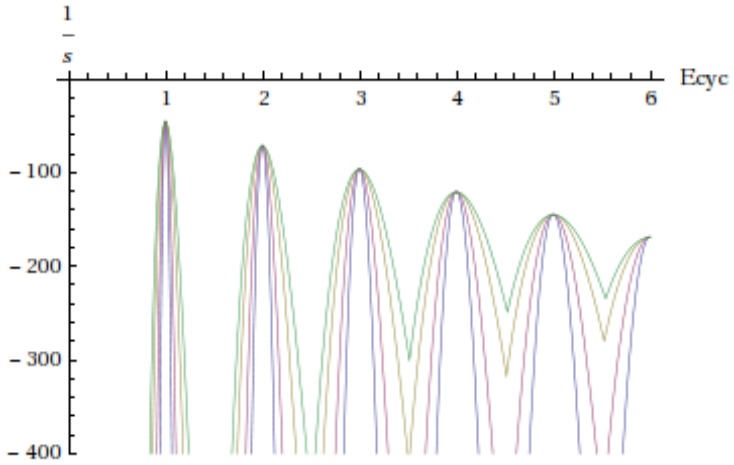

Figure 13: The plot is computed with Mathematica and shows the absorption probability per time of a photon propagating in the angle $\frac{\pi}{4}$ in logarithmic scale dependent of the energy in units of harmonic energy. The magnetic field is $B = 10^{15}$G and the five lines belong to different temperatures $T = 10^{8}$,$T = 10^{8.4}$, $T = 10^{8.8}$ and $T = 10^{9}$, where the resonances get broader while the temperature gets higher.

The Mathematica code to calculate $\frac{d\Gamma_{ab(\omega,\theta)}}{d\theta d\omega d\varphi dt}$ is:

```
mabssq[nin_, nout_, lin_, lout_, θ_, gen_, par_, perp_] :=
 Expand[2 charge^2 π^2 ħ c / (mass boltzmann T (gen * charge * B / (mass * c))^3 Cos[θ]^2) *
   e^(-(gen * charge * B / (mass * c))^2 Cos[θ]^2 ħ^2 / (4 mass c^2 boltzmann T)) *
   e^(-mass c^2 ((charge B / (mass c)) * (nout - nin - gen))^2 /
        (boltzmann T (gen * charge * B / (mass * c))^2 Cos[θ]^2))
   ((gen * charge * B / (mass * c))^2 / (c^3)) Sin[θ]
   (Expand[mabs[nin, nout, lin, lout, θ, (gen * charge * B / (mass * c)), par, perp]] /. ay → -i
   (Expand[mabs[nin, nout, lin, lout, θ, (gen * charge * B / (mass * c)), par, perp]] /. ay → i)
```

The following plots show the angle dependent absorption rate of a resonant photon. All transitions of the circular momentum quantum number are from 0 to 1. One can see the parallel part has changed its shape which is due to the fact that information is lost while the interaction process.

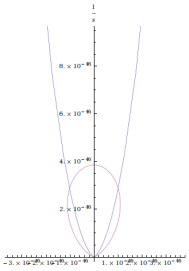

From Landau level 0 to 1

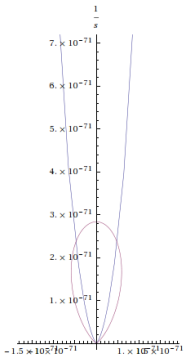

From Landau level 0 to 2

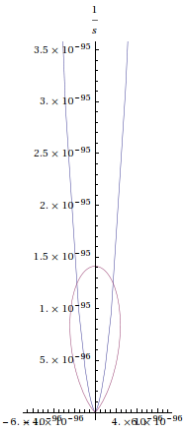

From Landau level 0 to 3

4.3 Absorption cross sections

The cross section defines a "surface" of the target particle and is therefore in units of area. This area divided by the complete target area gives the probability that a photon interacts with one of the point shape scattering centers. The differential cross section equals the transition rate divided by the photon number absolute squared (Merzbacher, 1998, 19.114).

$$\frac{d\sigma_{\mathrm{abs}}}{d\Omega} N_{(\vec{k})} = \Gamma \tag{132}$$

To evaluate the absorption cross section, one has to take all possible transitions into account. Here, all Landau protons are assumed in the ground state before the interaction. The absorption cross section can be evaluated by summing over all transition rates divided by the number of photons. Here the absorption rates from (Eq. 133) are used.

$$\begin{aligned}\frac{d\sigma_{\mathrm{abs}}}{d\Omega} = \frac{2e^2\pi^2}{m_{\mathrm{p}}k_BT}\frac{\hbar c}{\omega^3\cos\theta^2} e^{-\frac{\hbar^2}{4m_{\mathrm{p}}c^2k_BT}\omega^2\cos\theta^2} \sum_a\sum_b e^{-\frac{m_{\mathrm{p}}c^2}{k_BT\omega^2\cos\theta^2}\left(\frac{eB}{m_{\mathrm{p}}c}(b-a)-\omega\right)^2}\cdot \\ \cdot \Bigg| a_{\parallel}\cos\theta\langle\nu^b|e^{ik_xx}\partial_x|\nu^a\rangle + a_{\perp}\langle\nu^b|e^{ik_xx}\partial_y|\nu^a\rangle + \\ + i\left(\frac{\omega\cos\theta}{2c} + \frac{m_{\mathrm{p}}c}{\hbar\omega\cos\theta}\left(\frac{eB}{m_{\mathrm{p}}c}(b-a)-\omega\right)\right) a_{\parallel}\sin\theta\langle\nu^b|e^{ik_xx}|\nu^a\rangle\Bigg|^2\end{aligned} \tag{133}$$

The Mathematica code to calculate $\frac{d\sigma_{\mathrm{abs}}}{d\Omega}$ is:

```
mabssq[nin_, nout_, lin_, lout_, θ_, gen_, par_, perp_] :=
 Expand[2 charge^2 π^2 ħ c / (mass boltzmann T (gen * charge * B / (mass * c))^3 Cos[θ]^2) *
   e^(-(gen * charge * B / (mass * c))^2 Cos[θ]^2 ħ^2 / (4 mass c^2 boltzmann T)) *
   e^(-mass c^2 ((charge B / (mass c)) * (nout - nin - gen))^2 /
        (boltzmann T (gen * charge * B / (mass * c))^2 Cos[θ]^2))
   (Expand[mabs[nin, nout, lin, lout, θ, (gen * charge * B / (mass * c)), par, perp]] /. ay → -ⅈ
   (Expand[mabs[nin, nout, lin, lout, θ, (gen * charge * B / (mass * c)), par, perp]] /. ay → ⅈ)
```

To evaluate the absorption of photons it is important to know how many scattering centers the photon will meet on the way s, the particle density ρ_n is needed. The density in the rest-frame of the neutron star is approximated in chapter 2 to be around $\rho = 0.13 \cdot kg \cdot m^{-3}$. With assumed neutrality and the Proton mass m_{p}, the particle density of a homogeneous accretion column bottom reads:

$$\rho_{\mathrm{n}} = \frac{\rho}{m_{\mathrm{p}}} \approx 7.77223 \cdot 10^{25} \approx 10^{26} \tag{134}$$

The mean free path of a photon with angle θ and energy $\hbar\omega$ in strongly magnetized protons with the T can be evaluated via:

$$l_{(\omega,\theta,T)} = \left(\rho_{\mathrm{n}}\frac{d\sigma_{\mathrm{abs}(\omega,\theta,T)}}{d\Omega}\right)^{-1} \tag{135}$$

This gives as mean free path for a resonant photon with the angle $\frac{\pi}{4}$ for example:

$$l_{(\hbar\omega_{\mathrm{p}},\frac{\pi}{4},10^5)} \approx 10^{16}\mathrm{m} \tag{136}$$

$$l_{(\hbar\omega_{\mathrm{p}},\frac{\pi}{4},10^6)} \approx 10^{17}\mathrm{m} \tag{137}$$

$$l_{(\hbar\omega_{\mathrm{p}},\frac{\pi}{4},10^7)} \approx 10^{18}\mathrm{m} \tag{138}$$

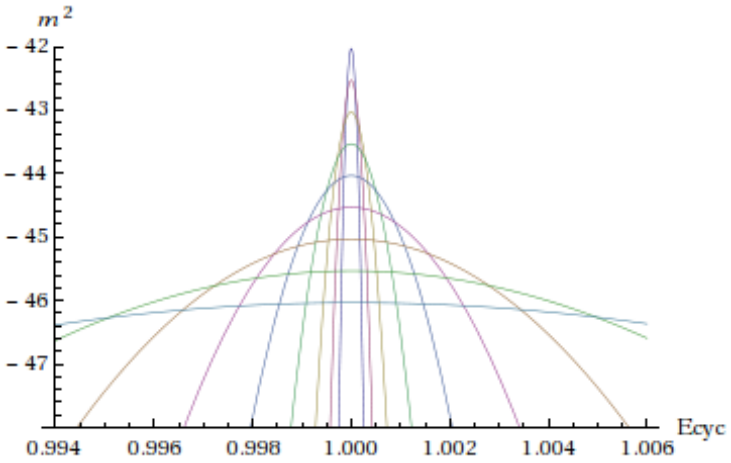

Figure 14: This plot shows in logarithmic scale the absorption cross section of a photon propagating in the angle $\frac{\pi}{4}$ relative to the magnetic field axis. The possible absorbers are Landau protons with the temperatures 10^5, $10^{5.5}$, 10^6, ..., 10^9 while the resonance gets lower and broader when the temperature gets higher.

5 Conclusions

The characteristics of the line forming region are investigated. The density of the accretion column bottom is found to be 0.13kgm^3 but with assumed $\dot{\rho}_h$ in the whole accretion stream. This value is estimated without density variations. The Geodesic equation is simplified and numerically integrated and the free-fall speed at the surface is $\sim 0.5c - 0 - 6c$, as expected. The column bottom in the accretion columns of neutron stars with 10^{15}G can be treated as small flat surface.
Due to the high proton mass, the thermal motion is negligible. At 10^9K we have $\frac{v}{c} \approx 10^{-4}$. To get rid of divergencies, the Landau proton is constructed as a wave package in the z-dimension in two different approaches.
I recalculated non relativistic quantum states in Cartesian coordinate space. The perturbation absorption matrix elements are calculated without dipole approximation. To automatize the integrations of the matrix elements, a Mathematica code is implemented. The differential absorption cross sections are evaluated. Mysteriously, the first resonance peak dominates the absorption rate. The angle dependence of the absorption rates are reproduced and show a small parallel part and a dominant perpendicular part. The interactions probability is strongly limited to the plane which is perpendicular to the magnetic field.
Finally, the mean free path of photons propagating through strongly magnetized protons is evaluated. The values suggest that photons with propagating parallel to the magnetic field are highly unlikely going to interact resonant with a landau proton. Resonant absorption should be expected in the plane perpendicular to magnetic field.

6 Appendix

6.1 Delta distribution

The delta distribution is not a function which one can write down. It's properties are constrained by definition.

$$\int_{-\infty}^{\infty} \delta_{(x'-x+x_0)} f_{(x')} dx' = f_{(x-x_0)} \tag{139}$$

If the delta distribution has a complicated function as argument, the distribution can be re-written in the way that:

$$\delta_{(g_{(x)})} = \sum_a \frac{\delta_{(x-x_a)}}{|g'_{(x_a)}|} \tag{140}$$

$$g_{(x_a)} = 0 \tag{141}$$

An important relation between the delta distribution and the sinc, which is used in this thesis reads:

$$\left(\frac{\sin{(x-x_0)t}}{(x-x_0)} \right)^2 = \pi t \delta_{(x-x_0)} \tag{142}$$

(42,4) in Landau & Lifschitz (b)

Another interesting relation connects the transition probability for infinite time with the transition probability rate.

$$\frac{1}{2\pi} \int_{-\infty}^{\infty} e^{-ik(x-x_0)} dk = \delta_{(x-x_0)} = \frac{d}{dt} t \delta_{(x-x_0)} = \frac{1}{2\pi} \frac{d}{dt} \int_{-\frac{t}{2}}^{\frac{t}{2}} e^{-ik(x-x_0)} dk \tag{143}$$

With this equation, one can equate the transition probability over infinite time with the transition probability rate.

6.2 Antisymmetric infinite integrals

It is important to notice, that many integrals one has to calculate are infinite integrals of antisymmetric functions. Antisymmetric functions are characterized by:

$$f_{(x)} = -f_{(-x)} \tag{144}$$

This means, the one half of the function integral is negatively equal to the other half. Proof:

$$\begin{aligned} \int f_{(x)} dx = \int_0^{\infty} f_{(x)} dx + \int_{-\infty}^{0} f_{(x)} dx = \int_0^{\infty} f_{(x)} dx - \int_0^{-\infty} f_{(x)} dx = \\ \int_0^{\infty} f_{(x)} dx - \int_0^{\infty} f_{(-x)} (-dx) = \int_0^{\infty} f_{(x)} dx - \int_0^{\infty} f_{(x)} dx = 0 \end{aligned} \tag{145}$$

QED

6.3 Gaussian Integrals

Often the only possible function used to be analytically integrate able is the Gaussian function. To simplify the calculus, we set $\frac{1}{b^2} = a$.

$$\int \frac{1}{b\sqrt{2\pi}} e^{-\frac{x^2}{2b^2}} dx = 1 \qquad \Longleftrightarrow \qquad \int \sqrt{\frac{a}{2\pi}} e^{-a\frac{x^2}{2}} dx = 1 \tag{146}$$

Taking into account that antisymmetric infinite integrals vanish, the gauss function itself is a symmetric function. Therefore integrals with an x with odd exponents are antisymmetric functions and become 0. In the representation with a one can easy see:

$$\int x^{2n} e^{-a\frac{x^2}{2}} dx = (-2)^n (\partial_a)^n \int e^{-a\frac{x^2}{2}} dx = \sqrt{2\pi}(-2)^n (\partial_a)^n a^{-\frac{1}{2}} \tag{147}$$

$$(\partial_a)^n a^{-\frac{1}{2}} = (\partial_a)^{(n-1)} \left(\frac{-1}{2}\right) a^{-\frac{3}{2}} = (\partial_a)^{(n-2)} \left(\frac{-1}{2}\right)\left(\frac{-3}{2}\right) a^{-\frac{5}{2}} = ... \tag{148}$$

$$\Longrightarrow$$

$$\sqrt{\frac{a}{2\pi}} \int x^{(2n)} e^{-a\frac{x^2}{2}} dx = \frac{(2n)!}{a^n 2^n n!} \tag{149}$$

Proof:

$$\int x^2 e^{-a\frac{x^2}{2}} dx = (-2)\partial_a \int e^{-a\frac{x^2}{2}} dx = \sqrt{\frac{2\pi}{a}} \frac{1}{a} \tag{150}$$

$$\begin{aligned} \int x^{2(n+1)} e^{-a\frac{x^2}{2}} dx &= (-2)\partial_a \int x^{2n} e^{-a\frac{x^2}{2}} dx = \\ &= (-2)\partial_a \left[\sqrt{\frac{2\pi}{a}} \frac{(2n)!}{a^n 2^n n!}\right] = (-2)\sqrt{2\pi}\frac{(2n)!}{2^n n!}\left(-n-\frac{1}{2}\right) a^{-n-\frac{3}{2}} = \\ &= \sqrt{\frac{2\pi}{a}} \frac{(2n)!(2n+1)(2n+2)}{a^{(n+1)} 2^n n!(2n+2)} = \sqrt{\frac{2\pi}{a}} \frac{(2n+2)!}{a^{(n+1)} 2^{(n+1)}(n+1)!} \end{aligned} \tag{151}$$

QED

It also makes sense, and is possible, to calculate Gaussian polynomials. Therefore, one can expand the exponential function, to get to the following form:

$$e^{-a\frac{x^2}{2}} e^{bx} = e^{(-a)\frac{x^2}{2} - (-a)2\frac{b}{2a} + (-a)\frac{b^2}{a^2}} e^{\frac{b^2}{2a}} = e^{\frac{b^2}{2a}} e^{-a\frac{\left(x-\frac{b}{a}\right)^2}{2}} \tag{152}$$

With that and the substitution, $\lambda = x - \frac{b}{a}$; $d\lambda = dx$, the integral can be split into summands:

$$\int x e^{-a\frac{(x-\frac{b}{a})^2}{2}} dx = \int \left(\frac{b}{a} + \lambda\right) e^{-a\frac{\lambda^2}{2}} d\lambda = \frac{b}{a}\int e^{-a\frac{\lambda^2}{2}} d\lambda + \int \lambda e^{-a\frac{\lambda^2}{2}} d\lambda = \frac{b}{a}\sqrt{\frac{2\pi}{a}} \tag{153}$$

The second in the sum is a antisymmetric infinite integral and vanishes. One can now try to generalize this for any x^n with the 1.Binomial formula (Bronstein et al., 2005, 1.36c):

$$\begin{aligned} \int x^n e^{-a\frac{x^2}{2}} e^{bx} dx = e^{\frac{b^2}{2a}} \int x^n e^{-a\frac{(x-\frac{b}{a})^2}{2}} dx = e^{\frac{b^2}{2a}} \int \left(\frac{b}{a} + \lambda\right)^n e^{-a\frac{\lambda^2}{2}} d\lambda = \\ e^{\frac{b^2}{2a}} \sum_{k=0}^{n} \binom{n}{k} \left(\frac{b}{a}\right)^{(n-k)} \int \lambda^k e^{-a\frac{\lambda^2}{2}} d\lambda \end{aligned} \tag{154}$$

To drop the polynomial terms, leading to antisymmetric integrals, one can now split odd and even n with $\xi_{(n)} = \frac{n}{2}$ if n is even and $\xi_{(n)} = \frac{n-1}{2}$ if n is odd.

$$\sqrt{\frac{a}{2\pi}} e^{\frac{b^2}{2a}} \sum_{k=0}^{\xi_{(n)}} \left(\begin{array}{c} n \\ 2k \end{array} \right) \left(\frac{b}{a}\right)^{(n-2k)} \int \lambda^{2k} e^{-a\frac{\lambda^2}{2}} d\lambda =$$

$$= e^{\frac{b^2}{2a}} \sum_{k=0}^{\xi_{(n)}} \frac{n!}{(2k)!(n-2k)!} \left(\frac{b}{a}\right)^{(n-2k)} \frac{(2k)!}{a^k 2^k k!} =$$

$$= e^{\frac{b^2}{2a}} n! \left(\frac{b}{a}\right)^n \sum_{k=0}^{\xi_{(n)}} \frac{1}{k!(n-2k)!} \left(\frac{a}{2b^2}\right)^k \quad (155)$$

$$\sqrt{\frac{a}{2\pi}} \int x^n e^{-a\frac{x^2}{2}} e^{bx} dx = e^{\frac{b^2}{2a}} n! \left(\frac{b}{a}\right)^n \sum_{k=0}^{\xi_{(n)}} \frac{1}{k!(n-2k)!} \left(\frac{a}{2b^2}\right)^k \quad (156)$$

This equation is equivalent to the formula (3.462,2) in Gradshtein & Ryshik (1981), and therefore verified. The Mathematica codes in this work use this formula to substitute manually.

7 References

Basko M.M., Sunyaev R.A., 1976, MNRAS 175, 395

Becker P.A., Wolff M.T., 2005, ApJ 630, 465

Becker P.A., Wolff M.T., 2007, ApJ 654, 435

Bronstein I.N., Semendjajew K.A., Musiol G., Mhlig H., 2005, Taschenbuch der Mathematik, Verlag Harri Deutsch, Frankfurt am Main, 6.,vollstaendig ueberarbeitet und ergaenzte auflage edition

Caballero I., Wilms J., 2012, Memsai 83, 230

Chaisson M., 2005, Astronomy Today, Pearson Prentice Hall, 5th ed. edition

Chandrasekhar S., 1931, ApJ 74, 81

Conte M., Palazzi M., Pusterla M., Turolla R., 2004, ArXiv High Energy Physics - Phenomenology e-prints

Daugherty J.K., Ventura J., 1978, Prd 18, 1053

Dirac P.A.M., 1947, The principles of quantum mechanics

Duric N., 2004, Advanced Astrophysics, Cambridge University Press

Esposito P., Rea N., Turolla R., et al., 2011, In: American Institute of Physics Conference Series.

Frank J., King A., Raine D., 2002, Accretion Power in Astrophysics, Cambridge University Press, 3rd edition

Fürst F., Kreykenbohm I., Pottschmidt K., et al., 2010, Aap 519, A37

Gradshtein I.S., Ryshik I.M., 1981, Summen-, Produkt- und Integral-Tafeln : deutsch und englisch = Tables of series, products, and integrals, Harvard Univ.Press, Cambridge

Heindl W.A., Rothschild R.E., Coburn W., et al., 2004, In: Kaaret P., Lamb F.K., Swank J.H. (eds.) X-ray Timing 2003: Rossi and Beyond, Vol. 714. American Institute of Physics Conference Series, p.323

Herold H., Ruder H., Wunner G., 1982, Astron. Astrophys. 115, 90

Hewish A., Bell S.J., Pilkington J.D.H., et al., 1968, Nat 217, 709

Hurley K., 2010, Mem. Societa Astronomica Italiana 81, 432

Ibrahim A.I., Swank J.H., Parke W., 2003, ApJL 584, L17

Iwasawa K., Koyama K., Halpern J.P., 1992, PASJ 44, 9

Johnson M.H., Lippmann B.A., 1949, Physical Review 76, 828

Kreykenbohm I., Mowlavi N., Produit N., et al., 2005, Astron. Astrophys. 433, L45

Landau L., Lifschitz E., , Klassische Feldtheorie, 12., überarbeitete edition

Landau L., Lifschitz E., , Quantenmechanik, 9. edition

Merzbacher E., 1998, Quantum mechanics; 3nd ed., Wiley, New York, NY

Meszaros P., 1992, High-Energy Radiation from Magnetized Neutron Stars, University Of Chicago Press

Metzger B.D., Giannios D., Thompson T.A., et al., 2011, MNRAS 413, 2031

Mihara T., Makishima K., Kamijo S., et al., 1991, ApJ 379, L61

Nakagawa Y.E., Mihara T., Yoshida A., et al., 2009, PASJ 61, 387

Oppenheimer J.R., Volkoff G.M., 1939, Physical Review 55, 374

Palmer D.M., Barthelmy S., Gehrels N., et al., 2005, Nat 434, 1107

Perna R., Pons J.A., 2011, ApJL 727, L51

Potekhin A.Y., 2010, Aap 518, A24

Rea N., Esposito P., 2011, In: Torres D.F., Rea N. (eds.) High-Energy Emission from Pulsars and their Systems., p. 247

Rea N., Zane S., Turolla R., et al., 2008, ApJ 686, 1245

Schönherr G., Wilms J., Kretschmar P., et al., 2007, Aap 472, 353

Shakura N.I., Sunyaev R.A., 1973, Aap 24, 337

Stöcker H., , Taschenbuch der Physik, year = 2004, Deutsch, Frankfurt am Main, 5., korrigierte aufl. edition

Thompson C., Duncan R.C., 1995, MNRAS 275, 255

Truemper J., Pietsch W., Reppin C., et al., 1978, ApJl 219, L105

Erklärung

Hiermit betätige ich, dass ich diese Arbeit selbsttändig und nur unter Verwendung der angegebanen Hilfsmittel angefertigt habe.

Bamberg,15.10.12

Maximilian Kriebel